Synthesis and characterization of rigid nanoporous hypercrosslinked copolymers for high surface area materials with potential hydrogen storage capabilities

Xu Zhou

Dissertation submitted to the Faculty of Virginia Polytechnic Institute and State University in partial fulfillment of the requirements for the degree of

MASTER OF SCIENCE
In
CHEMISTRY

S. Richard Turner, Chair
Harry W. Gibson
John Y. Walz

November 23, 2010
Blacksburg, Virginia

Keywords: Functionalized stilbene, N-substituted maleimide, hypercrosslinked, nanoporous, high surface area, hydrogen storage

Synthesis and characterization of rigid nanoporous hypercrosslinked copolymers for high surface area materials with potential hydrogen storage capabilities

Xu Zhou

ABSTRACT

Hydrogen storage remains a major technological barrier to the widespread adoption of hydrogen as an energy source. Organic polymers offer one potential route to useful hydrogen storage materials. Recently, Frechet and his coworkers described a series of hypercrosslinked polymers with high surface area and studied their surface properties and hydrogen storage capacities.[1-3] McKeown and his coworkers studied a class of materials termed Polymers of Intrinsic Microporosity (PIMs) which are also based on a "hypercrosslinked" concept.[4] We enchained N-substituted maleimide and functionalized stilbene alternating copolymers into a "hypercrosslinked system" to achieve high rigidity, high surface areas, high aromatic content and good thermal stability.

Hypercrosslinked copolymers of N-(3-methylphenyl)maleimide (3MPMI), 4-methyl stilbene (4MSTBB), vinylbenzyl chloride (VBC) and divinyl benzene (DVB) were synthesized. Scanning electron micrographs (SEM) show the copolymers are porous and some examples have shown surface areas over 1200 m^2/g. We have also found the

incorporation of 3MPMI and 4MSTBB improves the thermal stability and raises the glass transition temperature of the copolymer. However, the incorporation of 3MPMI and 4MSTBB decreases the hypercrosslinking density and therefore causes a decrease in the copolymer surface area. The systematic study of styrene (STR)– vinylbenzyl chloride (VBC) – divinyl benzene (DVB) networks indicates that a low density of chloromethyl groups leads to a decrease in surface area. Therefore, we are continuing to investigate other monomers, such as N-substituted maleimide and functionalized stilbene containing chloromethyl groups, in order to enhance thermal stability while maintaining surface area.

In order to increase the enthalpy of hydrogen adsorption and thus raise the temperature of hydrogen storage, the monomer N,N-dimethyl-N',N'-diethyl-4,4'-diaminostilbene (4,4' DASTB-3MPMI) which contains electron donating groups was incorporated into hypercrosslinked polymer particles. Hypercrosslinked polymer (4,4 ' DASTB-3MPMI)1.0(VBC)98.5(DVB).50 exhibits a surface area of 3257 m^2/g.

ACKNOWLEDGEMENTS

I would like to acknowledge my supervisor Dr. S. Richard Turner for his constant guidance and encouragement throughout my graduate study at Virginia Tech. I would also like to thank Dr. Harry W. Gibson and Dr. John Y. Walz for serving on my research committee and their advice and help on my research. I would like to thank Dr. Paul A. Deck for his guidance on my graduate program. I would also like to thank Dr. Gordon T. Yee for offering valuable advice on graduate school.

I would like to thank Dr. Frantisek Svec for the measurement of surface area and helpful advice on the hydrogen storage project. I would like to thank Dr. Myongbae Lee in Dr. James E. McGrath's group, for his help on TGA, DSC instruments. I would also like to thank Thomas F. Cromer for the SEM training.

To my lab mates in general, thank you for the daily help and discussion. Special thanks to Yi Li and LaShonda Cureton Williams, for their support and friendship. I am grateful to Ms. Mary Jane Smith for her patience and assistance. I would also like to acknowledge Ms. Angie Miller and Ms. Tammy Jo Hiner for their assistance.

To my family, my parents and my loving grandmother, thank you for your endless love. I could not have gone so far without your support. To my dearest friends, Renjie Han and Xiaowei Zhai, thank you for always being there and giving me the strength to keep moving forward.

TABLE OF CONTENTS

LIST OF FIGURES

LIST OF TABLES

LIST OF SCHEMES

CHAPTER 1. INTRODUCTION

1.1 Introduction

CO_2 emission from fossil fuel is considered the main factor causing global warming. The growth rate of CO_2 emissions was 3.5% per year for the period of 2000-2007, which is almost a fourfold the increase from 0.9% per year in 1990-1999.[5] On the other hand, as the global economy increases, energy demand is increasing while available fossil fuels are going to decrease dramatically in a few decades. The great challenge we face is keeping the balance between economic development and environmental protection that is, meeting energy demands while protecting the environment.

Hydrogen is clean and renewable. Low molecular weight and high molar heat of combustion (the amount of energy released in burning completely one mole of substance) make hydrogen one of the best candidates to replace fossil fuels.[6] The term "hydrogen economy" coined in 1970 is a proposed system using hydrogen as a carrier of energy. However, "hydrogen storage is the critically missing link to a future hydrogen economy".[7] In the past few decades, hydrogen storage has aroused scientists' interest and become a popular topic (Figure 1-1). How to store hydrogen efficiently, both costs and safety are big obstacles we have to solve. The requirements for on-board hydrogen storage are particularly strict.

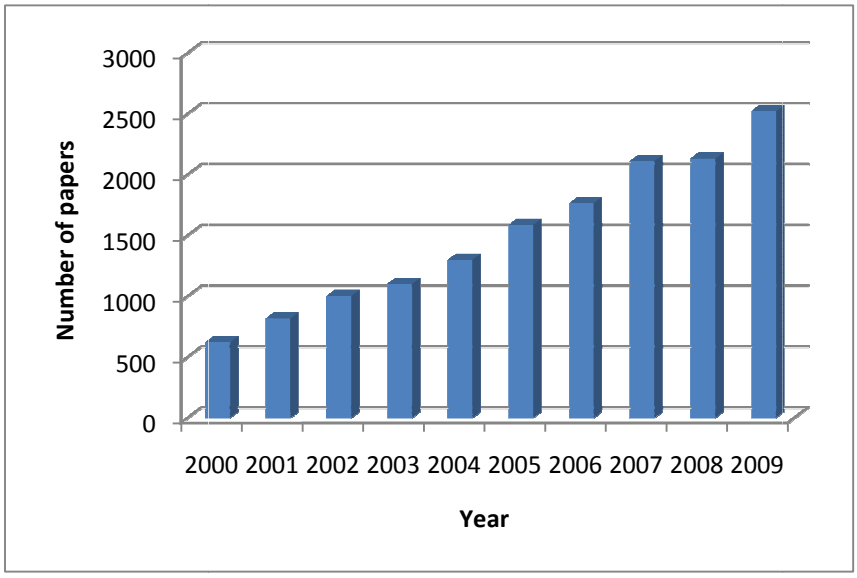

Figure 1-1 Graph showing increasing number of papers that feature the term "hydrogen storage" in their titles, abstracts or keywords (source: SciFinder)

The U. S. Department of Energy has set up targets for hydrogen storage systems considering capacity, cost, durability, charging rate, safety, etc.[8] Table 1-1 shows part of the targets for on-board hydrogen storage systems. The 2010 DOE gravimetric and volumetric targets are 6 wt% and 45g H_2/L respectively. However, in addition to storage materials, the storage system includes pressure containment valves, cooling systems etc. which will lower down the storage capacity for the whole system. Therefore, in order to achieve the system level required from DOE, the storage capacity must be greater than 6 wt% for the material.

Table 1-1. DOE Technical Targets: On-Board Hydrogen Storage Systems[8]

Storage Parameter	Units	2007	2010	2015
System Gravimetric Capacity: Usable, specific-energy from H_2 (net useful energy/max system mass)	kWh/kg	1.5	2	3
	(kg H_2/kg system)	(0.045)	(0.06)	(0.09)
System Volumetric Capacity: Usable energy density from H_2 (net useful energy/max system volume)	kWh/L	1.2	1.5	2.7
	(kg H_2/L system)	(0.036)	(0.045)	(0.081)
Storage system cost (& fuel cost)	$/kWh net	6	4	2
	($/kg H_2)	(200)	(133)	(67)
	$/gge at pump	---	2-3	2-3

*kWh: kilowatt hour; gge: gasoline gallon equivalent

A large number of materials has been designed and their properties for hydrogen storage have been studied. There are two major types of storage methods for solid-state hydrogen storage: physical storage and chemical storage. Metal hydrides, which have been studied intensely in the past four decades, are the classic examples of chemical storage. Under appropriate conditions, hydrogen reacts with metals to form metal hydrides, which can be stored as solids. However, inherent thermodynamic energy inefficiency and slow kinetics limit their applications in the hydrogen economy.[3] Nanoporous materials are good alternatives to physically store hydrogen since they avoid issues associated with metal hydrides. Table 1-2 summarizes the hydrogen

storage capacity and surface area of some common nanoporous materials.

Table 1-2. Comparison of some currently investigated hydrogen storage materials

Material	Storage level, wt%	Temperature/ pressure	Surface area, m^2/g	References
Metal-organic framework (MOF)	7-11	77 K, 2.5-8 MPa	4400-4600	[9-11]
Polymers with intrinsic microporosity (PIMs)	0.7-2.7	77 K, 0.1-1 MPa	580-1065	[12-14]
Carbon materials	1.7-6.9	77 K, 0.1-2.0 MPa	-	[3,15-17]
Crosslinked porous polymers	0.4-1.3	77 K, 0.12 MPa	359-1206	[3]
Hypercrosslinked polymers	1.3-5.4	77 K, 0.12-8 MPa	1930	[1-3,18,19]

1.2 Carbon materials

1.3.1. Activated carbon

Activated carbon (AC) is composed of small graphite crystallites and amorphous carbon.[20] Due to its low cost and convenient availability in industry, application of AC for hydrogen storage has received a lot of research attention.[20-22] Hydrogen adsorption of AC is physisorption which normally follows the Langmuir adsorption isotherm.

1.3.2. Carbon nanotubes

Carbon nanotubes (CNT) include "single-wall nanotubes" (SWNT) and "multi-wall nanotubes" (MWNT). Due to different formations, CNT can also be divided into "armchair", "zigzag", and "chiral" types (Figure 1-2).[20]

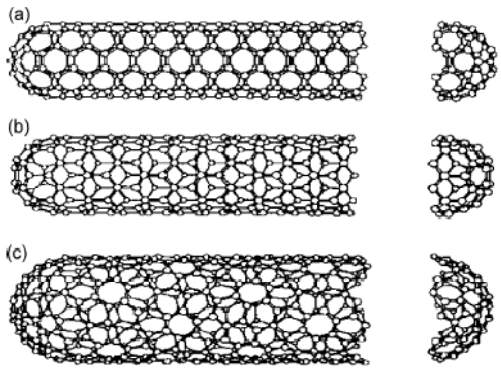

Figure 1-2. Different SWNT structures: (a) armchair, (b) zigzag, and (c) chiral[23]

Hydrogen uptake of CNT has a linear relationship with tube diameter because the uptake is proportional to the surface area (one layer adsorption).[20] Hydrogen storage values depend on many parameters such as structure, structural defects, geometry, storage pressure, temperature, etc.[24] It was reported that hydrogen storage capacity of multi-wall nanotubes (MWNT) at room temperature can reach 6.3 wt% at 14.8 MPa[25]

1.3 Covalent Organic Frameworks (COFs)

Covalent organic framework (COFs), with high porosity and low density, are composed of organic units linked by strong covalent bonds (C-C, C-O, B-O, and Si-C).[26,27] Yaghi and coworkers designed and synthesized covalent organic frameworks: COF-1 and COF-5 which exhibit high thermal stability (to temperature up to 500 to 600℃),

permanent porosity, and high surface areas (711 and 1590 m^2/g).[28] COF-1 (Scheme 1-1) and COF-5 can be synthesized by condensation reaction of boronic acids.[28]

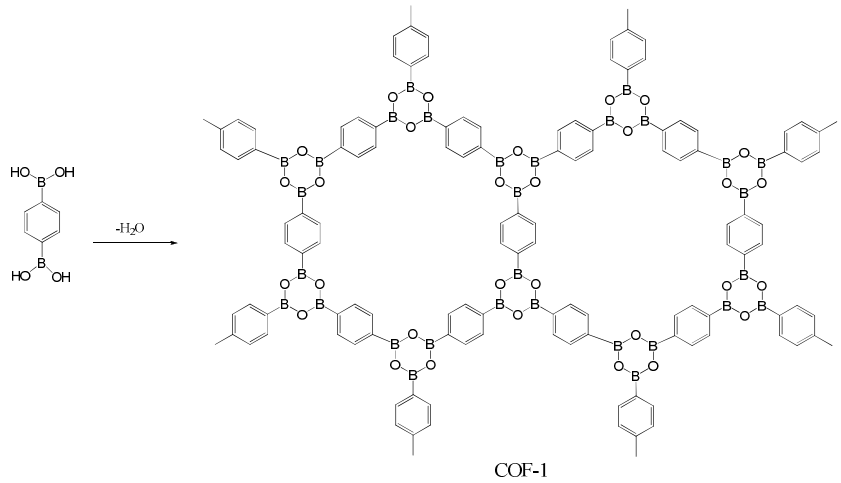

Scheme 1-1. Condensation reaction of boronic acid used to produce COF-1

Moreover, they introduced three-dimensional covalent organic frameworks (3D COFs) in another publication.[27] These materials have high thermal stabilities (400-500℃), high surface areas (up to 4210 m^2/g), and low densities (0.17 g/cm^3). Furthermore, grand canonical Monte Carlo (GCMC) simulations were used to predict hydrogen storage capacities of COFs.[26] They found that hydrogen storage capacity in three dimentional COFs is 2.5-3 times higher than that in two-dimensional COFs. Thus, 3D COFs are more promising candidates for hydrogen storage.

1.4 Metal - Organic Frameworks (MOFs)

Metal-organic frameworks are crystalline inorganic-organic hybrid materials which have low density, high porosity, crystallinity, and large specific surface area.[29,30] The combination of inorganic and organic components allows the structural properties of

MOFs to be controlled, thus increasing the volume of pores or increasing the energy of hydrogen binding.[29,31]

Metal-organic frameworks, good candidates for hydrogen storage, have been intensively studied. The structure of MOFs can be described as a lattice construction. Rigid organic fragments link like rods of the lattice while inorganic clusters are located in the nodes (Figure 1-3).[29]

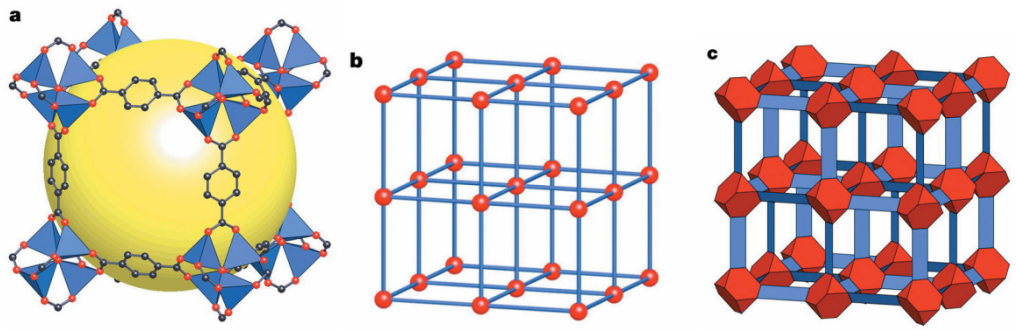

Figure 1-3. a, The MOF-5 structure shown as ZnO_4 tetrahedra joined by benzene dicarboxylate linkers to give an extended 3D cubic framework. b, The topology of the structure shown as a ball-and-stick model. c, The structure shown as the envelopes of the $(OZn_4)O_{12}$cluster and benzene dicarboxylate (BDC) ion.[32]

In the past years, about 11000 MOFs have been made.[29,30,32-34] There are two types of organic linkers in MOFs, charged and uncharged. Carboxylate ions and heterocyclic ligands are most important charged and uncharged linkers, respectively.[29] And Cu(II), Mn(II), Zn(II), Ni(II), and lanthanide ions are frequently used metal ions.[29]

Although high surface areas are obtained with by MOFs (~ 4000 m^2/g), they are not utilized efficiently for hydrogen storage.[35] Current MOFs present moderate uptake

volumes but low gravimetric adsorption capacity. Moreover weak interaction to retain hydrogen is another issue to prevent MOFs storing hydrogen at ambient temperature.[36] Many MOFs have been found to be extremely sensitive to air or other impurities which degrade the hydrogen adsorption capacities.

1.5 Organic polymers for hydrogen storage

Organic polymers have several advantages as hydrogen storage materials.[37] They can be made solely from light elements such as carbon, hydrogen, and oxygen. Hence they are better candidates for hydrogen transportation compared to other materials such as MOFs. Secondly, a large number of available synthetic routes not only make synthesis possible but also make them tunable. Moreover, polymer technology is scalable so that they are fewer knowledge barriers to commercial production. In this section, the main classes of organic polymers for hydrogen storage are described.

1.5.1. Polymers with intrinsic microporosity (PIMs)

Polymers with intrinsic microporosity (PIMs) are highly rigid and contorted macromolecules which pack space inefficiently to achieve high internal surface area (Figure 1-4).[4,38,39] Moreover, synthetic diversity is another advantage of PIMs.[38] PIMs can be prepared by using benzodioxane formation between suitable monomers as insoluble network polymers or as solvent processable no-network polymers.[38,39]

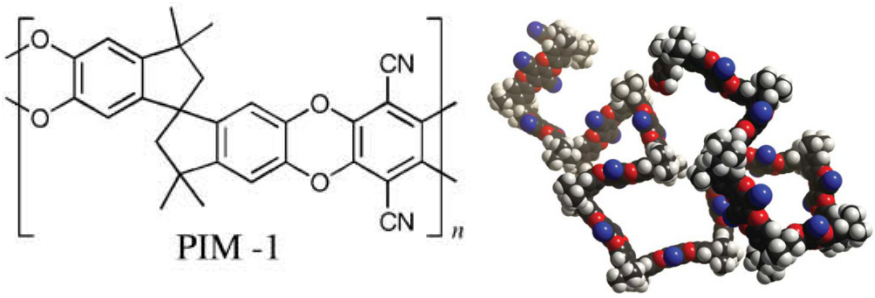

Figure 1-4. Molecular structure of PIM-1 (left)[38] and molecular model of a small fragment of PIM-1 (right)[4]

McKeon et al. synthesized rigid polymer networks by incorporating extended aromatic components in order to mimic the graphene sheets of activated carbons.[4] They first chose the phthalocyanine macrocycle as the aromatic unit;[40] however, previous phthalocyanine network polymers were non-porous due to strong non-covalent interactions.[41] To solve this problem, they found that highly rigid and nonlinear linking groups between the phthalocyanine subunits would prevent loss of microporosity. [4] The synthesis scheme of phthalocyanine-based network polymers of intrinsic microporosity (Pc-Network-PIMs) is shown below (Scheme 1-2). In the following year, they continued to design and study properties of PIMs.[38,42]

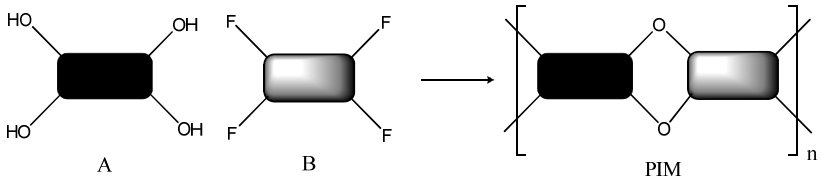

Scheme 1-2. Synthesis scheme of PIM, i. Monomer A, Monomer B, K_2CO_3, DMF.[4]

A publication from McKeon et al. in 2010 summarized a large number of PIMs.[43] Monomer structures and the characterization of pore structure were discussed. In order

to prevent micropore structure from collapsing, linking groups should not have significant rotational freedom. However, PIMs have a general disadvantage because of the multistep synthesis that are likely to present significant challenges as scale up targets.

1.5.2. Hypercrosslinked polymers

In 1969, Davankov and co-workers introduced a novel method of synthesis of porous polystyrene networks.[44] This method includes highly swelling linear polystyrene chains in solvent and post-crosslinking by Friedel-Crafts reaction. Since 1970s, Davankov-type resins have become one of the most well-studied hypercrosslinked materials.[44-47] Besides polystyrene networks, they also extended their study on other polymeric highly crosslinked network which process high porosity as well.[48]

In 2006, Sherrington et al. reported a convenient method to synthesize Davankov-type hypercrosslinked resin beads (Scheme 1-3).[49] By using gel-type and permanently porous poly(divinylbenzene-co-vinylbenzyl chloride) (DVB-VBC) precursor resins without external electrophiles, hypercrosslinked resins with surface area up to ~2000 m^2g^{-1} were synthesized.

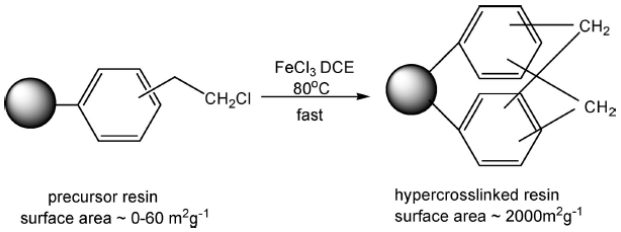

Scheme 1-3. Synthesis scheme of hypercrosslinked poly(DVB-VBC) without external electrophiles[49]

In the same year, Svec et al. studied the properties and hydrogen storage capacity of some commercially available porous polymer beads (Table 1-3). Among the commercial materials, Hypersol-Macronet MN200 and Lewatit EP63 resins exhibited the highest adsorption capacity for hydrogen (1.3 wt% at 0.12 MPa, 77.3 K).

Table 1-3. List of commercial resins, their properties, and their ability to store hydrogen[1]

Trade name	Composition	Surface area(m^2/g)[a]		H_2 capacity
		a	b	(wt %)[b]
Amberlite XAD4	poly(styrene-co-divinylbenzene)	1060	425	0.8
Amberlite XAD16	poly(styrene-co-divinylbenzene)	770	336	0.6
Hayesep N	poly(divinylbenzene-co-ethylenedimethacrylate)	460	247	0.5
Hayesep B	polydivinylbenzene modified with polyethyleneimine	570	290	0.5
Hayesep S	poly(divinylbenzene-co-4-vinylpyridine)	510	254	0.5
Wofatit Y77	poly(styrene-co-divinylbenzene)	940	573	1.2
Lewatit EP63	poly(styrene-co-divinylbenzene)	1206	664	1.3
Lewatit VP OC 1064	poly(styrene-co-divinylbenzene)	810	377	0.7
Hypersol-Macronet MN200	hypercrosslinked polystyrene	840	576	1.3
Hypersol-Macronet MN100	amine functionalized hypercrosslinked polystyrene	600	477	1.1
Hypersol-Macronet MN500	sulfonated hypercrosslinked polystyrene	370	266	0.7

[a] Calculated from nitrogen adsorption using the BET equation (a) and hydrogen adsorption using the Langmuir equation (b). [b] Hydrogen storage capacity at a pressure of 0.12 MPa.

Moreover, they utilized the synthesis method modified by Sherrington et al. to synthesize a series of hypercrosslinked polymers based mostly on simple styrenic monomers for hydrogen storage via free radical suspension polymerization followed by Friedel-Crafts reaction (Scheme 1-4).[1] Hypercrosslinked polystyrene made from this gel (chloromethylstyrene-co-divinylbenzene) exhibits BET surface area of 1930 m^2/g and 1.5 wt% hydrogen uptake at 0.12 MPa and 77.3 K. In their later work, hydrogen storage capacities of 3.8 and 5.4 wt% at 4.5 and 8.0 MPa were achieved using the same polystyrene material.[18]

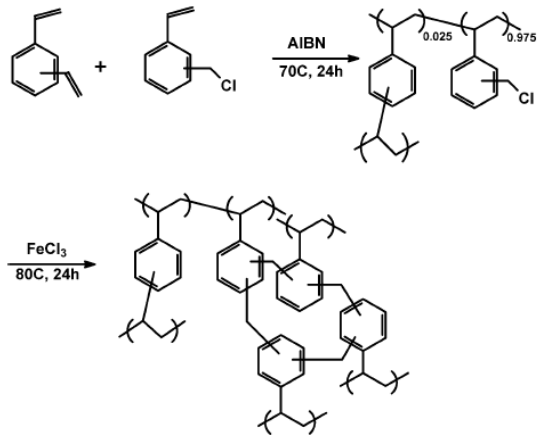

Scheme 1-4. Reaction scheme for synthesis of hypercrosslinked polystyrene from gel (chloromethylstyrene-co-divinylbenzene)[1]

Another publication from Svec et al. reported the preparation of novel nanoporous polyaniline, with specific surface areas exceeding 630 m^2/g and hydrogen storage capacity of 2.2 wt% at 3.0 MPa and 77 K.[2] Nanoporous polyanilines can be prepared by hypercrosslinking polyaniline with difunctional reagents, diiodoalkanes or formaldehyde (Scheme 1-5). A difunctional reagent is used to compensate for the

limited reactivity of polyaniline and both reagents can lead to formation of rigid crosslinks. The porous properties are affected by the concentration of polyaniline in the reaction mixture.

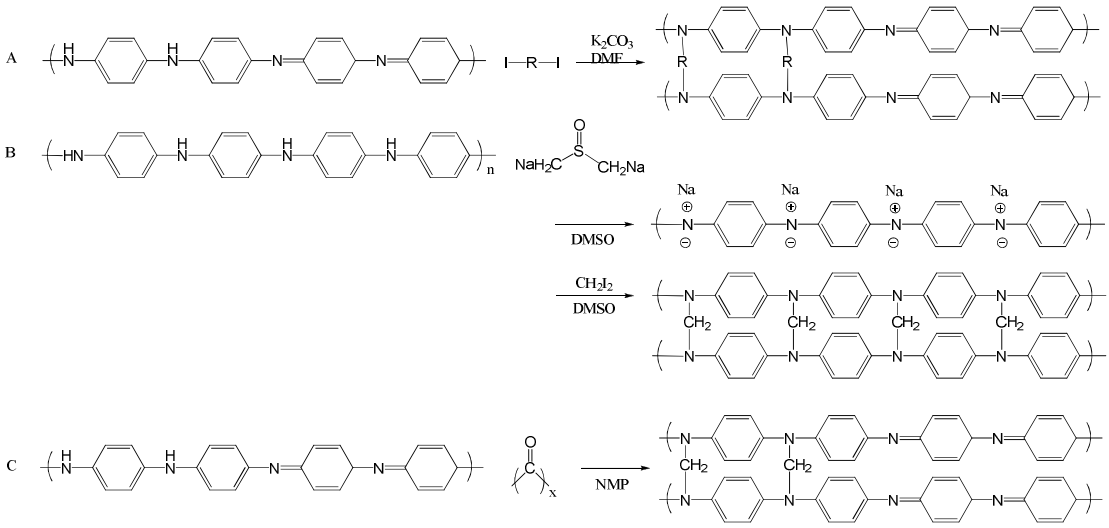

Scheme 1-5. Simplified reaction schemes showing preparation of hypercrosslinked polyaniline: (A) using single step crosslinking with diiodoalkanes, (B) dimethylsulfoxide-assisted two-step crosslinking with diiodomethane, (C) crosslinking with paraformaldehyde.[2]

For common nanostructured materials, enthalpies of hydrogen adsorption are 4-7 kJ/mol while the suggested value for hydrogen storage at room temperature is 15 kJ/mol.[3] Theoretical work has suggested that electron rich aromatic groups should have significantly higher enthalpy of hydrogen adsorption.[2] The hypercrosslinked polyanilines Svec et al. synthesized exhibit remarkably high enthalpies of hydrogen adsorption of up to 9.3 kJ/mol. These results indicate that incorporation of electron rich aromatic groups in the polymer has great promise in delivering polymeric materials that

can store hydrogen at or near room temperature, which may make hydrogen storage at room temperature more feasible.

In 2007, Cooper et al. synthesized a series of hypercrosslinked polymer networks by self-condensation of bis(chloromethyl) monomers.[37] These materials exhibit BET surface areas of up to 1904 m^2/g (Langmuir surface areas 2992 m^2/g), gravimetric storage capacity as high as 3.68 wt% at 15 bar and 77.3 K. Figure 1-5 shows the monomers used for synthesis of networks:

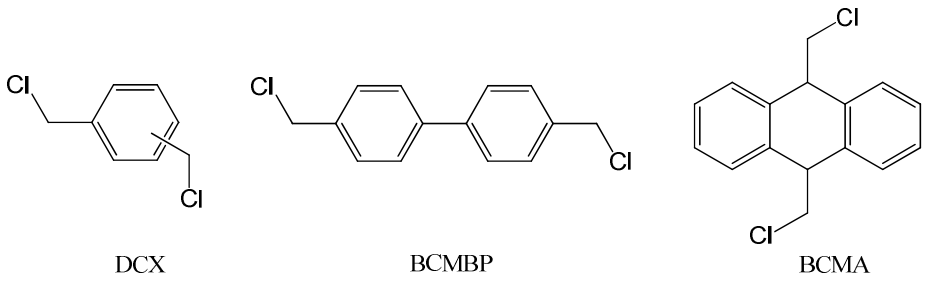

Figure 1-5. Monomers used for the synthesis of the hypercrosslinked polymer network. DCX: Dichloroxylene (ortho-, meta-, and para-isomers). BCMBP: 4,4'-Bis(chloromethyl)-1,1'-biphenyl. BCMA: Bis(chloromethyl) anthracene.[37]

In this publication, varying reaction conditions, pore structures and H_2 sorption properties of the materials were studied. They conclude that materials made by self-condensation of bis(chloromethyl) monomers such as DCX and BCMBP have better gas storage properties. Two factors, level of cross-linking and design of the rigid monomer unit, are both important to the porosity and hydrogen storage capacity of polymer networks.

1.6 Research objectives

A publication by Frechet and Svec describes hypercrosslinked polymers prepared by suspension polymerization to give high surface areas and hydrogen storage capacities.[1] On the other hand, McKeown and his coworkers studied a class of materials termed Polymers of Intrinsic Microporosity (PIMs).[4,38-42] In their research, rigid, aromatic components are incorporated in order to pack space inefficiently and thus increase internal surface area.

In the study of nanostructured polymers for hydrogen storage, several aspects play important roles. The rigidity of polymer backbone is crucial to the high surface area and good pore structure. In the study of polyaniline network from Svec et al., longer, more flexible crosslinkers used in synthesis results in lower surface area of networks.[2] The decrease in surface area is hypothesized to result from pore structure collapse due to the flexible linker when the solvent is removed rapidly from the polymer during the drying step (Scheme 1-6).[2,3]

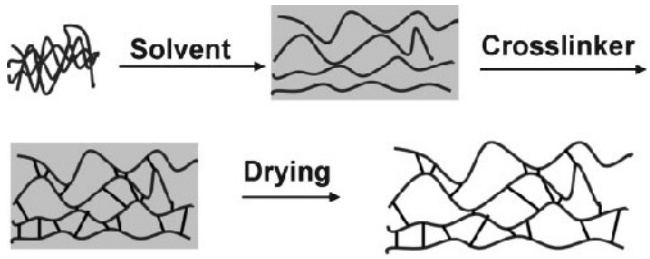

Scheme 1-6. Scheme of the hypercrosslinking process.[2]

Since in metal free all-aromatic materials the H_2-aromatic group interaction is the driving force for adsorption, the nature of the aromatic groups plays an important role

in the process.[50,51] Theoretical studies suggest that the incorporation of electron-donating substituents on the aromatic ring should lead to a stronger H_2-aromatic group interaction.[52] Therefore, electron-donating groups increase the enthalpy of hydrogen adsorption which permit an increased temperature for reversible hydrogen adsorption from 77 K to a higher temperature which could approach the DOE goal of room temperature.[2]

Based on the concepts discussed above, we have incorporated functionalized stilbene and N-substituted maleimide alternating copolymer sequences into the hypercrosslinked polystyrene network that have been reported by Svec et al..[1]. These stiffened highly functionalized aromatic structures based on functionalized stilbene alternating copolymers were expected to have high free volumes, high aromatic content, and high surface area and the stiffer chain should be a barrier to the collapse of the nanopores during the formation process. The stiffened alternating copolymers also have excellent thermal stability as evidenced by no thermal decompositions below 350 ^{o}C and no observable glass transition temperatures. Moreover, incorporation of specific functional groups such as electron donating groups along the backbone might increase hydrogen adsorption enthalpy and further enhance hydrogen storage capacity.

A two-step procedure reported by Frechet and Svec was used to synthesize hypercrosslinked polymers.[1] N-substituted maleimides and functionalized stilbene monomers along with vinylbenzyl chloride (VBC) and divinyl benzene (DVB) were polymerized via suspension polymerization initiated by azobisisobutyronitrile (AIBN)

and formed lightly crosslinked precursor particles. The precursor particles were then swollen in dichloromethane (DCM) and post-crosslinked via Friedel-Crafts reaction in the present of $FeCl_3$ to yield hypercrosslinked polymer networks (Scheme 1-7).

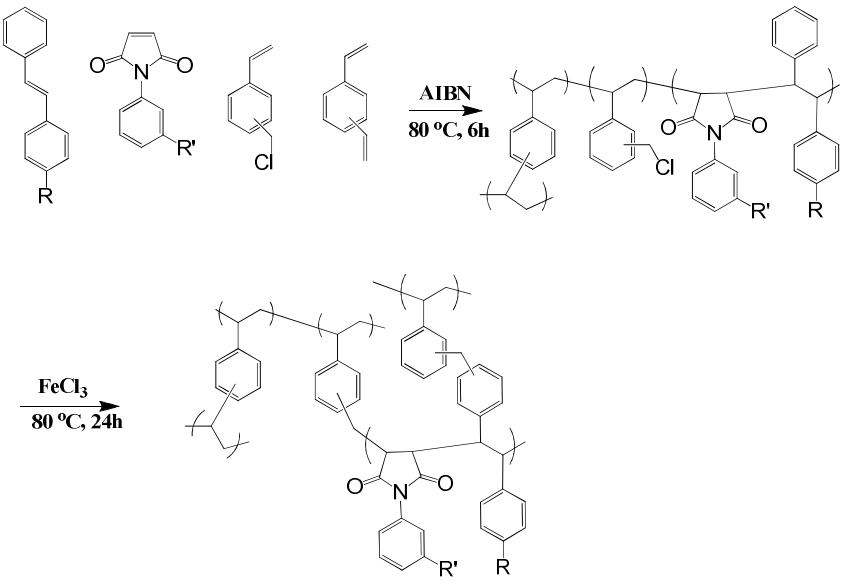

Scheme 1-7. Synthesis scheme for hypercrosslinked polymer network

In our study, nuclear magnetic resonance (NMR), Fourier transform infrared spectroscopy (FT-IR) and elemental analysis were utilized to characterize monomers, lightly crosslinked precursors and hypercrosslinked polymer networks. Scanning electron microscopy (SEM) was used to probe the porous structures of both precursors and hypercrosslinked polymers. Also, thermal properties of the polymer networks were studied using thermalgravimetric analysis (TGA) and differential scanning calorimetry (DSC). Surface area and hydrogen uptake were measured at the Molecular Foundry at Lawrence Berkeley in California.

1.4.1. Functionalized stilbene and N-substituted maleimide copolymer with vinylbenzyl chloride (VBC) and divinylbenzene (DVB) networks

Functionalized stilbene - N-substituted maleimide alternating copolymer was incorporated into VBC-DVB network. The amount of functionalized stilbene - N-phenyl maleimide copolymer was varied in order to study the effect on the thermal properties, surface area and hydrogen storage capacity of polymers. The functionalized stilbene - N-substituted maleimide copolymer segment was expected to enhance the rigidity of the polymer backbone, thus maintaining the pore structure during the drying step to yield high surface area networks.

1.4.2. Functionalized stilbene and N-substituted maleimide copolymer with N-allylmaleimide networks

In this study, N-allylmaleimide was used to substitute for divinylbenzene as the crosslinker. This was done in order to replace DVB with the higher T_g maleimide. It was previously shown that a high concentration of the allylic double bond survives the alternating cross propagation, but the pendant allylic group should still serve as a crosslinking site in the suspension polymerization step.[53] Based on the fundamentals of alternating copolymerizating, the copolymers should have a lower crosslinked density than those prepared from divinylbenzene, since the divinyl benzene would be expected to participate more efficiently in the cross-propagation alternation step.

1.4.3. Chloromethyl stilbene and chloromethyl N-phenyl maleimide copolymer with divinyl benzene networks

Chloromethyl stilbene and chloromethyl N-phenyl maleimide copolymer were designed and synthesized to substitute for vinylbenzyl chloride which serves as a crosslinking agents in the particle formation crosslinking step (Scheme 1-8). The objective of this approach was to eliminate the low T_g vinylbenzyl chloride from the backbone and to supply the requisite chloromethyl group via higher T_g units. The rigidity of the polymer backbone is expected to increase without decreasing the density of chloromethyl groups.

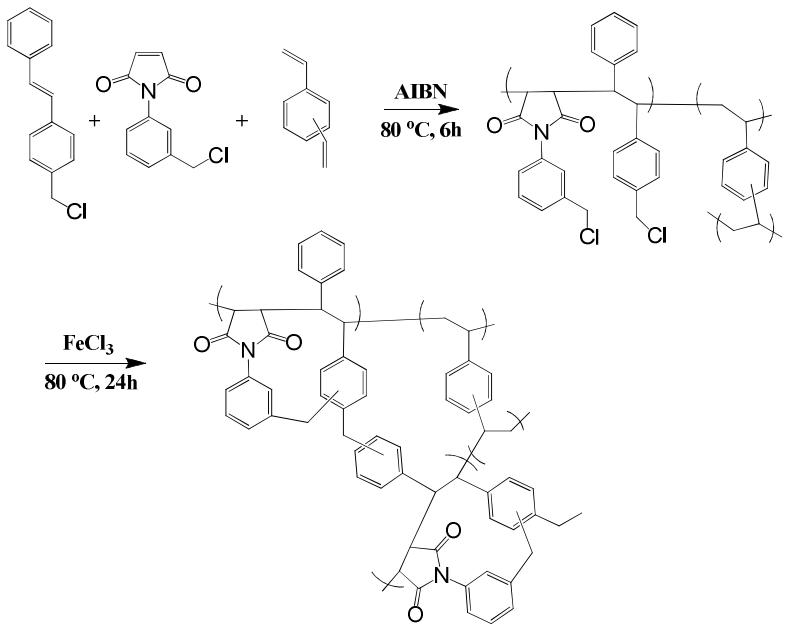

Scheme 1-8. Synthesis scheme for hypercrosslinked poly(4-chloromethyl stilbene-3-chloromethyl phenyl maleimide-divinyl benzene) network (4CMSTB-3CMPMI-DVB)

CHAPTER 2. EXPERIMENTAL

2.1. Materials

4-Methylbenzyl chloride (Aldrich, 98%), triethyl phosphite (Aldrich, 98%), benzaldehyde (Aldrich, ≥99%), ^{t}BuOK (Aldrich, 1.0M solution in THF), maleic anhydride (Aldrich, 99.0%), toluene (Fisher, certified ACS), *m*-toluidine (Aldrich, 99%), acetic anhydride (Aldrich, 98%), sodium acetate (Aldrich, anhydrous), 1, 2-dimethoxy ethane (Fluka, puriss), allyl amine (Acros, 98%+), benzyl chloride (Aldrich, 99%), terephathaldicarbaldehyde (Aldrich, 99%), $LiAlH_4$ (Aldrich, 95%), 3-nitrobenzylalcohol (Aldrich, 98%), methanol (Fisher, HPLC grade), sodium borohydride (MP, 98-99%), dichloromethane (Aldrich, 99%), $ZnBr_2$ (Aldrich, puriss), dry benzene (Aldrich, anhydrous, 99.8%), hexamethyldisilazane (Acros, 98%), 1,2-dichloroethane (Aldrich, ≥99%), $FeCl_3$ (Aldrich, 97%), Raney nickel (Aldrich, Raney®2800, slurry in water), poly(vinyl alcohol) (Aldrich, 87-89% hydrolyzed), sodium chloride (Fisher, certified ACS crystaline) were used as purchased. AIBN was recrystallized from methanol.

2.2. Monomer synthesis

2.3.1. Synthesis of (E)-4-methyl stilbene

(*E*)-4-Methyl stilbene was synthesized via the Wittig-Horner reaction using 4-methyltoluene(diethylphosphonate) and benzaldehyde (Scheme 2-1).[54] To synthesize 4-methyltoluene(diethylphosphonate), 4-methylbenzylchloride (15.0 g, 107 mmol) and

triethyl phosphite (70.9 g, 427 mmol) were stirred in a 250 ml flask and heated to 160 ^{o}C for 24 hours. The remaining triethyl phosphite was removed by vacuum distillation at 80 ^{o}C under 0.2 mmHg to afford a colorless liquid (27.1 g, 100%).

4-Methyltoluene(diethylphosphonate) (27.1 g, 112 mmol) and benzaldehyde (11.9, 112 mmol) in dry THF (60 ml) were stirred in a 250 ml round bottom flask cooled in an ice bath. ^{t}BuOK (1.0 M in THF, 120 mL) was then added dropwise. The solution formed was stirred at room temperature for an additional 24 hours after which it was poured into water (500 ml). The product which precipitated from the solution was filtered and washed with water and vacuum dried overnight to yield (*E*)-4-methyl stilbene (white crystalline solid, 18.7 g, 86%). ^{1}H NMR ($CDCl_3$, 500 MHz) δ ppm: 7.52 – 7.08 (m, 11H), 2.37 (s, 3H). Melting point: 116 – 118 ^{o}C (lit.[55]:118 – 120 ^{o}C).

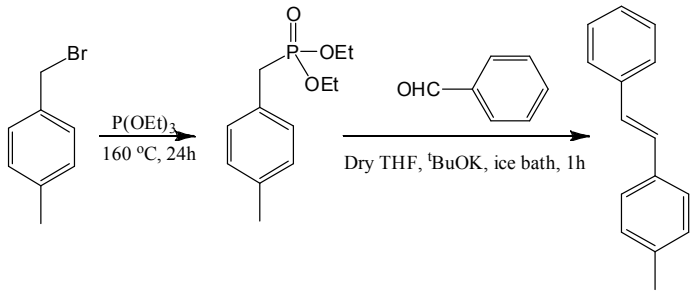

Scheme 2-1. Synthesis of (E)-4-methyl stilbene

2.3.2. Synthesis of N-(3-methylphenyl)maleimide

N-(3-Methylphenyl)maleimide have synthesized from a two step reaction (Scheme 2-2). The second step of the reaction used a modified literature method.[56] To synthesize *N*-(3-methylphenyl)maleamic acid, maleic anhydride (10.0 g, 102 mmol) and toluene (8 ml) were stirring in a 100 ml flask. *m*-Toluidine (11.1 g, 102 mmol) was added

portion wise. During the addition, 15 ml toluene was added to maintain a good slurry consistency, after which the mixture was refluxed for 15 minutes. The product precipitated from solution was filtered warm and vacuum dried for 24 hours to afford light yellow solid (19.63 g, 94%). ^{1}H NMR (DMSO, 400 MHz) δ ppm: 10.27 (s, 1H), 7.43 – 6.87 (m, 4H), 6.42 (d, 1H), 6.26 (d, 1H), 2.23 (s, 3H).

A mixture of *N*-(3-methylphenyl)maleamic acid (17.6 g, 85.9 mmol), acetic anhydride (43.8 g, 429 mmol) and anhydrous sodium acetate (3.52 g, 42.9 mmol) was heated at 100 ^{o}C for 6 hours. The reaction mixture was cooled and poured in ice water. The crude product was then washed with ice water and vacuum distillated (62 ^{o}C, 0.2 mmHg) to afford N-(3-methylphenyl)maleimide (yellow liquid, 15.1 g, 94%). Then the crude product was purified by column chromatography (silica gel, hexane-ethyl acetate = 5:1). The first band afforded pure product as a yellow liquid (6.19, 41%) ^{1}H NMR (DMSO, 500 MHz) δ ppm: 7.36 (m,1H), 7.22 - 7.10 (m, 5H), 2.34 (t,3H).

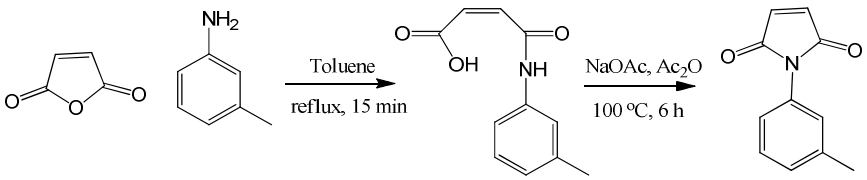

Scheme 2-2. Synthesis of N-(3-methylphenyl)maleimide

2.3.3. Synthesis of N-allyl maleimde

N-Allyl maleimide was prepared in a two-step reaction following literature methods (Scheme 2-3).[57,58] First *N*-allyl maleamic acid was synthesized by dissolving maleic

anhydride (6.57g, 67 mmol) in dimethoxyethane (5 ml) in a 100 ml round bottom flask cooled in an ice bath. While the mixture was stirring, allyl amine (5.0 ml, 67 mmol) was added drop-wise over 45 minutes. The mixture was stirred for another 1.5 hour at room temperature. A white precipitate was filtered, washed with cold water, and recrystalized with water. The product was vacuum dried at 40 ^{o}C overnight to afford white needles (4.00 g, 39%). ^{1}H NMR (DMSO, 500 MHz) δ ppm: 9.13 (s, 1H), 6.40 (d, 1H), 6.26 (d, 1H), 5.82 (m, 1H), 5.20 - 5.10 (m, 2H), 3.81 (m, 3H).

N-Allyl maleamic acid (4.00 g, 25.8 mmol) was heated at 130 ^{o}C for 30 minutes. The reaction mixture was then purified by column chromatography (silica gel, hexane-ethyl acetate = 2:1) to afford milky liquid (0.60 g, 18%; Lit[58]: 20%). ^{1}H NMR (DMSO, 500 MHz) δ ppm: 7.05 (s, 2H), 5.79 (m,1H), 5.09 – 5.01 (m, 2H), 4.00 (m, 2H). Melting point: 44 - 46 ^{o}C (lit.[58]: 47 ^{o}C).

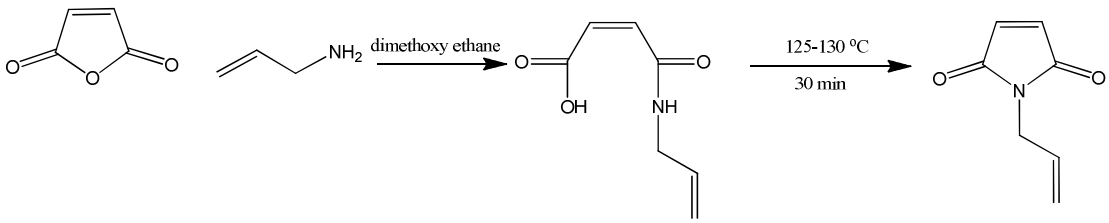

Scheme 2-3. Synthesis of *N*-allyl maleimde

2.3.4. Synthesis of (E)-4-(Chloromethyl)stilbene

(*E*)-4-(Chloromethyl)stilbene was prepared by a four-step reaction (Scheme 2-4). To synthesize benzyl(diethylphosphonate), benzyl chloride (28.8 g, 168 mmol) and triethyl phosphite (70.9 g, 672 mmol) were first stirred in a 500 ml flask and heated at

160 ^{o}C for 24 hours. The remaining triethyl phosphite was removed by vacuum distillation at 80 ^{o}C under 0.2 mmHg to afford colorless liquid (38.4 g, 100%). ^{1}H NMR ($CDCl_3$, 500 MHz) δ ppm: 7.32-7.23 (m, 5H), 4.00 (m, 4H), 3.17 (s, 1H), 3.12 (s, 1H), 1.23 (t, 6H).

(*E*)-4-Stilbenecarbaldehyde was synthesized following a previous literature method[59]. Benzyl (diethylphosphonate) (5.3 g, 23 mmol) and terephathaldicarbaldehyde (9.3 g, 69 mmol) were dissolved in dry THF (300 ml) under nitrogen gas in an ice bath. ^{t}BuOK (1.0 M in THF, 25.5 ml) was added drop-wise using an addition funnel over 1 hour. The solution was stirred for 3 hours at room temperature. Then the solution was evaporated to dryness and the product was purified by column chromatography (silica gel, DCM-hexane = 1:1, second band) to afford white solid (2.67g, 55%). ^{1}H NMR (DMSO, 500 MHz) δ ppm: 9.99 (s, 1H), 7.92 (d, 2H), 2.84 (d, 2H), 7.66 (d, 2H), 7.54 – 7.33 (m, 5H).

(*E*)-4-Stilbenemethanol was synthesized as follows: $LiAlH_4$ (0.12 g, 3.2 mmol) was dissolved in dry THF (30 ml) under nitrogen gas. (*E*)-4-stilbenecarbaldehyde (0.55 g, 2.6 mmol) dissolved in dry THF (15 ml) was added in several portions. The mixture was then heated at 70 ^{o}C for 5 hours. The reaction was quenched by slowly adding water (5 ml). After filtration, the filtrate was washed with 15% NaOH solution and water. After drying with anhydrous magnesium sulfate, the solution was evaporated to afford light yellow solid (0.86 g, 100%). ^{1}H NMR (DMSO, 500 MHz) δ ppm: 7.60 (m, 4H), 7.37 – 7.23 (m, 7H), 5.20 (t, 1H), 4.49 (d, 2H).

(*E*)-4-(Chloromethyl)stilbene was prepared following a modified literature method.[60] (*E*)-4-Stilbenemethanol (2.34 g, 11.2 mmol), pyridine (0.5 ml), $SOCl_2$ (3 ml) and dry CH_2Cl_2 (150 ml) were placed in a flask under nitrogen. The mixture was stirred for 7 hours cooled with an ice bath. The mixture was evaporated to dryness and purified by column chromatography (silica gel, hexane - CH_2Cl_2 = 2:1) to afford a yellow solid (2.93, 100%). ^{1}H NMR (DMSO, 500 MHz) δ ppm: 7.61 (m, 4H), 7.45 – 7.28 (m, 7H), 4.77 (s, 2H). Melting point: 113 – 114 ^{o}C (lit.[61]: 116 ^{o}C).

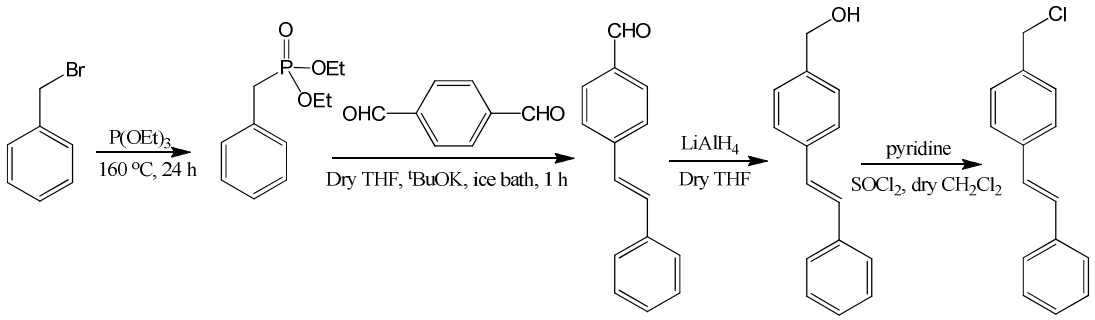

Scheme 2-4. Synthesis of (*E*)-4-(chloromethyl)stilbene

2.3.5. Synthesis of N-(3-chloromethylphenyl)maleimide

3-Aminobenzyl alcohol was prepared following a literature method (Scheme 2-5).[62] Raney nickel (0.059 g, 10 mol%) was added to 100 ml flask cooled in an ice bath, and washed with methanol for three times. 3-Nitrobenzyl alcohol (1.53 g, 10 mmol) and 20 ml methanol were then added. Sodium borohydride (0.76g, 20 mmol) was slowly added. The reaction mixture was stirred for one hour. The catalyst was filtered off, washed with methanol and immediately immersed in water to avoid combustion. The filtrate was evaporated to dryness. Dichloromethane (20 ml) and water (20 ml) were used to

dissolved the residue. Additional dichloromethane was used to extract the water. The combined organic layer was dried and evaporated to dryness to afford beige solid (0.78 g, 64%). ^{1}H NMR ($CDCl_3$, 400 MHz) δ ppm: 6.90 (t, 1H), 6.52 – 6.43 (m, 3H), 4.93 (m, 3H), 4.33 (d, 2H).

N-(3-Hydroxymethylphenyl)maleimide was synthesized following a literature method.[63] Maleic anhydride (4.26 g, 43.4 mmol) and 3-aminobenzyl alcohol (5.35 g, 43.4 mmol) in dry benzene (30 ml) was stirred in a 100 ml two-neck flask for 4 hours at 50 °C. After adding $ZnBr_2$ (9.77 g, 43.4 mmol, the mixture was heated at 80 °C. Hexamethyldisilazane (HMDS; 12.9 g, 0.0781 mol) in dry benzene (10 mL) was then added slowly over 30 minutes. The mixture was refluxed for an hour and cooled to room temperature. Then it was poured into 0.5 N HCl solution and extracted by ethyl acetate. The organic extract was washed with saturated $NaHCO_3$ solution, water and dried with anhydrous magnesium sulfate. The solution was evaporated to dryness and purified by column chromatography (silica gel, hexane : ethyl acetate = 3:1, first band) to afford yellow solid (4.43 g, 50%, Lit[63]: 62%). ^{1}H NMR ($CDCl_3$, 500 MHz) δ ppm: 7.45 – 7.37 (m, 4H), 6.85 (s, 2H), 4.75 (d, 2H), 1.72 (m, 1H).

To synthesize *N*-(3-chloromethylphenyl)maleimide, *N*-(3-hydroxymethyl phenyl)maleimide (3.63 g, 17.9 mmol) was dissolved in $SOCl_2$ (15 ml). The mixture was stirred for 2 hours. The solvent was removed. The residue was extracted with ethyl acetate, washed with $NaHCO_3$ solution and water and then dried with anhydrous $MgSO_4$ to afford yellow liquid (3.89g, 98%). ^{1}H NMR ($CDCl_3$, 400 MHz) δ ppm: 7.47

- 7.33 (m, 4H), 6.86 (s, 2H), 4.61 (s, 2H).

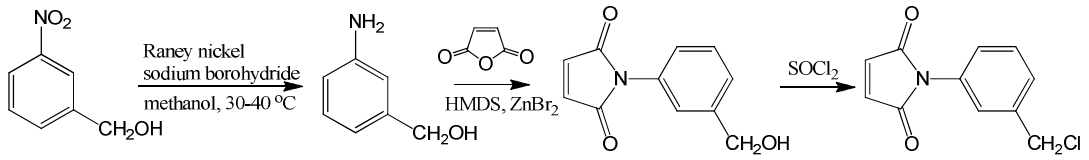

Scheme 2-5. Synthesis of N-(3-chloromethylphenyl)maleimide

2.3.6. Synthesis of t-butyl hypochlorite

t-Butyl hypochlorite was prepared following a literature method.[64] Commercial bleach (50 ml) was stirred in an 250 ml flask which was cooled in an ice bath. t- Butyl alcohol (2.96 g, 40 mmol) and glacial acetic acid (2.64 g, 44 mmol) were added. The mixture was stirred for 3 minutes. The organic layer which formed as a yellow liquid was separated, washed with sodium carbonate solution, water, and dried with anhydrous $MgSO_4$ to afford yellow liquid (0.81, 19%) ^1H NMR ($CDCl_3$, 400 MHz) δ ppm: 1.29 (m, 9H).

2.3.7. Chlorination of (E)-4-methylstilbene using N-chlorosuccinimide

(*E*)-4-Methylstilbene (1.00 g, 5.15 mmol), *N*-chlorosuccinimide (0.69 g, 5.15 mmol) and 2,2'-azobis(isobutyronitrile) (0.0051 g, 3 wt%) were dissolved in dry benzene (10 ml). The mixture was stirred at reflux for 4 hours. A white precipitate formed and filtered. The yellow liquid residued was washed with water, dried with $MgSO_4$ and

vacuum dried. NMR was that of starting material and showed the desired chlorination reaction was unsuccessful.

2.3.8. Chlorination of (E)-4-methyl stilbene using SO_2Cl_2

(*E*)-4-Methylstilbene (0.500 g, 2.58 mmol), SO_2Cl_2 (0.418 g, 3.09 mmol), 2,2'-azobis(isobutyronitrile) (0.0008 g) were stirred at 80 ^oC under N_2 for 30 minutes. A yellow viscous liquid was formed. Four different spots including the one from starting material were shown on the thin layer chromatography (TLC) plate. Column chromatography was not ideal for purifying the product because the product and by-products have similar polarity. Therefore, this synthetic route was abandoned.

2.3.9. Chlorination of (E)-4-methylstilbene using t-Butyl hypochlorite

(*E*)-4-Methylstilbene (0.500 g, 2.58 mmol), t-butyl hypochlorite (0.308 g, 2.84 mmol), 2,2'-azobis(isobutyronitrile) (0.0024 g, 3 wt%) were stirred in dry benzene (5 ml) at 80 ^oC for 2 hours to yield yellow oil. The absence of protons associated with the chloromethyl group indicates that the desired product was not formed. This synthetic route was abandoned.

2.3. Polymer synthesis

2.3.1. Functionalized stilbene - N-substituted maleimide copolymer

Functionalized stilbene - N-substituted maleimide copolymers were synthesized via

free radical solution polymerization initiated by AIBN in THF. For copolymer (4MSTB)50(3MPMI), 4MSTB (0.90 g, 4.6 mmol), 3MPMI (0.87g 4.6 mmol), and AIBN (5.3 mg, 0.3 wt%) were dissolved in 10 ml THF in a glass bottle under N_2. The mixture was heated at 60 ^oC for 6 hours. Then the polymer was precipitated in hexane, filtered and vacuum dried for 24 hours at 50 ^oC.

2.3.2. Hypercrosslinked polymers

Hypercrosslinked polymers were prepared following a modified literature procedure (Scheme 2-6).[1,37] For preparation of a hypercrosslinked polymer of (4MSTB-3MPMI)40(VBC)40(DVB)20, (*E*)-4-methyl stilbene (0.673 g, 3.47 mmol), N-(3-methylphenyl)maleimide (0.649 g, 3.47 mmol), vinylbenzyl chloride (0.529 g, 3.47 mmol) and divinylbenzene (0.225 g, 1.73 mmol) were added to a three-neck, 250 ml round bottom flask equipped with a mechanical stirrer, gas inlet, and condenser. Additionally, to the mixture, poly (vinyl alcohol) (0.195 g, 9.4 wt%), sodium chloride (0.858 g, 41.4 wt%), and DI water (30 ml) were added. The polymerization was initiated with 2,2'-azobis(isobutyronitrile) (0.0104 g, 0.5 wt%). The mixture was stirred under N_2 at 80 ^oC for 6 hours. The polymer beads were filtered, extracted with methanol and diethyl ether via Soxhlet extractor, and dried under vacuum at 50 ^oC for 24 hours to yield a white solid (1.115 g, 54%).

The precursor (0.847 g) was swollen in 1,2 dichloroethane (10 ml) for a few hours. Then $FeCl_3$ (0.468 g) was added and the mixture was heated at 80 ^oC for 18 hours. The hypercrosslinked polymer was extracted with THF and vacuum dried at 50 ^oC for 24

hours to afford a brown powder (0.505 g).

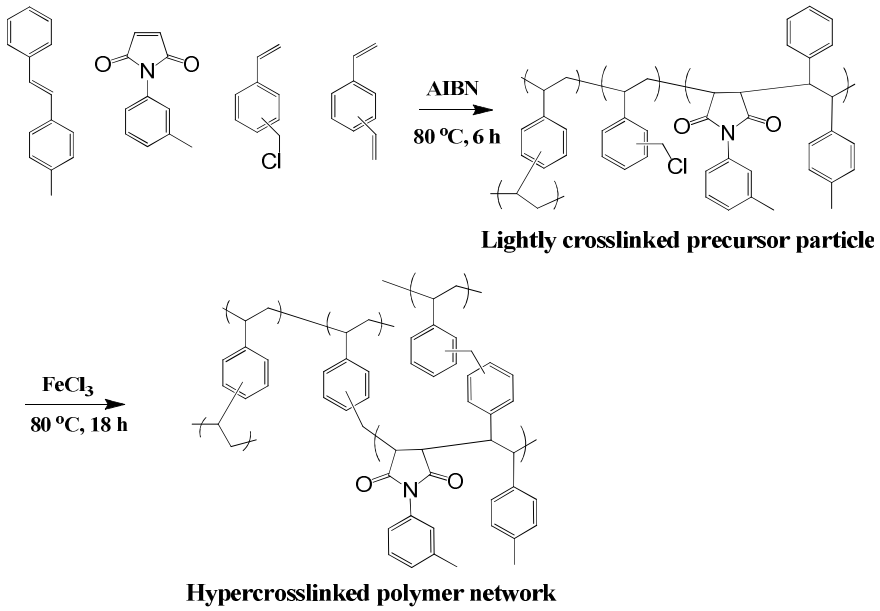

Scheme 2-6. Synthesis of hypercrosslinked polymer

2.4. Characterization methods

2.4.1. Nuclear Magnetic Resonance (NMR)

Proton nuclear magnetic resonance (^{1}H NMR) was utilized to confirm the chemical composition of monomers and non-crosslinked polymers. $CDCl_3$-d and $DMSO_{d6}$ were used as the solvents for NMR. ^{1}H NMR was obtained on Varian Utility 400 MHz, Inova 400 MHz or JOEL EclipsePlus 500 MHz spectrometers at 25 °C.

2.4.2. Fourier Transform Infrared Spectroscopy (FT-IR)

Infrared spectra were obtained to confirm the incorporation of N-substituted maleimide into the polymer networks. Monomers, lightly crosslinked precursor particles and hypercrosslinked polymer were measured using a Midac FTIR spectrometer.

2.4.3. Thermogravimetric Analysis (TGA)

Thermogravimetric Analysis (TGA) was employed to study the thermal stability of polymer precursors and hypercrosslinked polymers using TA instrument model Q5000. Samples were heated from 30 ^{o}C to 600 ^{o}C at a heating rate of 10 ^{o}C/min under nitrogen.

2.4.4. Differential Scanning Calorimetry (DSC)

Thermal transitions such as glass transition (T_g) were obtained by Differential Scanning Calorimetry (DSC) using a TA instrument model Q1000. Samples were measured using heat/cool/heat method at heating and cooling rate of 10 ^{o}C under nitrogen.

2.4.5. Scanning Electron Microscope (SEM)

SEM was employed to obtain pictures of the micro structure for both polymer precursors and hypercrosslinked polymers. All materials were coated with gold using a Sputter Coater S150B instrument at 40 mA under argon for 3 minutes. SEM micrographs were obtained using the ISI Scanning Electron Microscope.

2.4.6. Brunauer-Emmett-Teller Surface Area

The Brunauer-Emmett-Teller (BET) surface areas were obtained from nitrogen adsorption/desorption isotherms at 77 K using a Micromeritics ASAP 2020 or an ASAP 2010 surface area and porosimetry analyzer (Norcross, GA) at Lawrence Berkeley National Laboratory.

CHAPTER 3. RESULT AND DISCUSSION

3.1. Monomer synthesis

N-Phenyl maleimide monomers were synthesized via the formation of maleamic acid followed by ring close reaction. *N*-(3-Methylphenyl)maleimide, *N*-allyl maleimide and *N*-(3-chloromethylphenyl)maleimide were synthesized successfully and confirmed by ^{1}H NMR.

(*E*)-4-Methylstilbene was synthesized via the Wittig-Horner reaction. In order to synthesize (*E*)-4-(Chloromethyl)stilbene, different approaches of chlorination of (*E*)-4-methylstilbene were utilized. Chlorination of (*E*)-4-methylstilbene using N-chlorosuccinimide or t-butyl hypochlorite as chlorinating agent was unsuccessful. ^{1}H NMR and TLC (thin layer chromatography) show no reaction occurred. An alternative chlorinating agent, SO_2Cl_2, was then utilized. However, several products were shown by TLC which are likely chlorinated chloromethyl stilbene, by products dichloromethylstilbene and trichloromethylstilbene. Therefore, this method was abandoned and a known method, chlorinating (*E*)-4-stilbenemethanol to form (*E*)-4-(chloromethyl)stilbene was used.

3.2. Functionalized stilbene - N-substituted maleimide copolymers and characterization

In order to confirm the formation of the functionalized stilbene - N-substituted maleimide alternating copolymer sequence, copolymers (4MSTB)50(3MPMI)50 and (4CMSTB)50(3CMPMI)50 were synthesized in a free radical solution polymerization.

Elemental analysis data indicates that the (4MSTB)50(3MPMI)50 copolymer was

formed. According to the calculation, the actual composition is (4MSTB)44(3MPMI)56 (Table 3-1). Table 3-2 shows elemental analysis data of (4CMSTB)50(3CMPMI)50 copolymer. The composition is (4CMSTB)40(3CMPMI)60. This indicates the maleimide can add to itself.

Table 3-1. Elemental analysis data of (4MSTB)50(3MPMI)50 copolymer

Element	Theory, %	Found, %	
	(4MSTB)50(3MPMI)50	(4MSTB)44(3MPMI)56	
C	82.76	78.78	78.91
H	5.04	5.96	6.08
N	3.71	4.18	4.18

Table 3-2. Elemental analysis data of (4CMSTB)50(3CMPMI)50 copolymer

Element	Theory, %	Found, %	
	(4CMSTB)50(3CMPMI)50	(4CMSTB)40(3CMPMI)60	
C	69.98	65.56	65.45
H	4.38	4.38	4.32
N	3.14	3.72	3.84

3.3. Synthesis and characterization of hypercrosslinked polymer particles

In the process of preparing hypercrosslinked polymers, free radical suspension polymerization was involved to form lightly crosslinked precursors. In suspension polymerization organic monomer droplets are dispersed in water in the present of

stabilizer under mechanical agitation to form spherical particles in size range of 50-500μm (Figure 3-1).[65] Suspension polymerization has several advantages. The presence of dispersion medium (e.g.,water) makes the reaction temperature easier to control. Compared to bulk processes, suspension polymerization requires milder reaction conditions. Higher purity can be obtained from suspension polymerization compared to emulsion polymerization.[66]

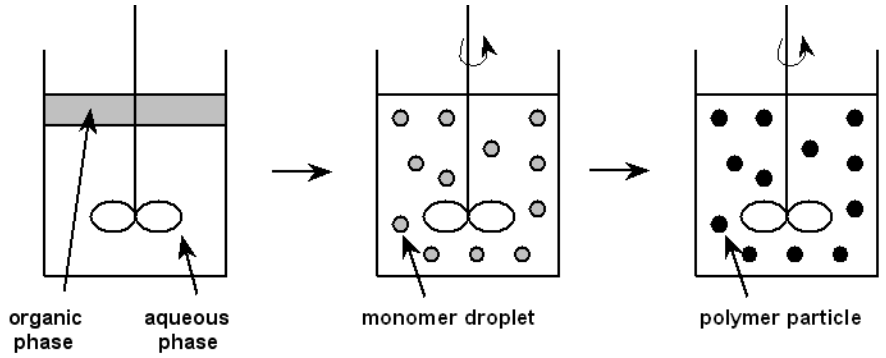

Figure 3-1. Schematic representation of a suspension polymerization[67]

Hypercrosslinked polymers containing (*E*)-4-methylstilbene (4MSTB), *N*-(3-methylphenyl)maleimide (3MPMI), vinylbenzyl chloride (VBC) and divinylbenzene (DVB) were synthesized successfully via free radical suspension polymerization followed by Friedel-Crafts reaction. Hypercrosslinked polymers containing 4MSTB, 3MPMI, VBC and N-allyl maleimide (AMI) were synthesized using the same synthesis strategy. Hypercrosslinked polymer (VBC)98(DVB)2 containing 98 % VBC and 2 % DVB was synthesized and used as the control for comparing hypercrosslinked 4MSTB-3MPMI-VBC-DVB and 4MSTB-3MPMI-VBC-AMI polymers.

FT-IR was used to confirm incorporation of 3MPMI into the precursor particle prepared with free radical suspension polymerization. Stretching adsorption bands of the

carbonyl group were observed around 1700 cm^{-1} for precursor particles containing 3MPMI monomer (Figure 3-2). For the control precursor of (VBC)98(DVB)2, no carbonyl group band was observed.

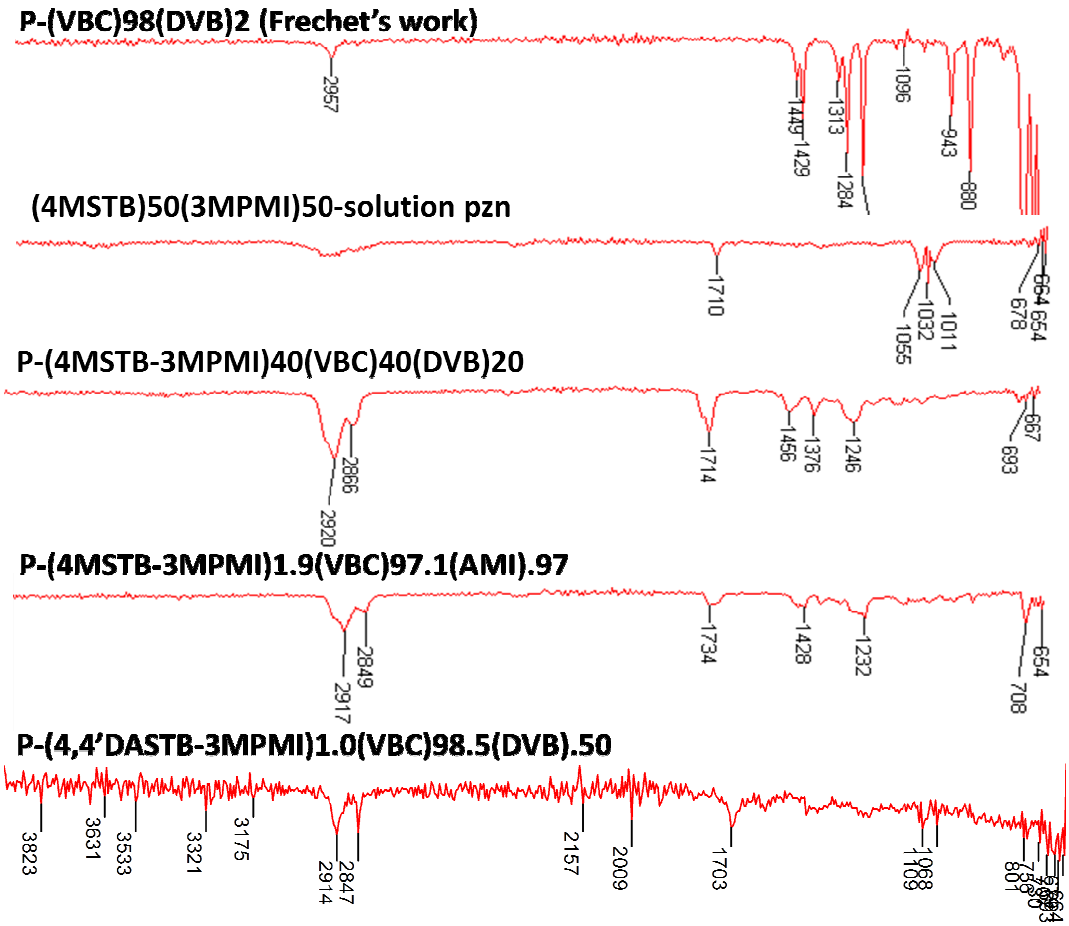

Figure 3-2. IR spectra of (VBC)98(DVB)2-precursor, (4MSTB)50(3MPMI)50-solution polymerization, (4MSTB-3MPMI)40(VBC)40(DVB)20-precursor, (4MSTB-3MPMI)1.9(VBC)97.1(AMI)0.97-precursor and (4,4' DASTB-3MPMI)1.0(VBC)98.5(DVB).5-precursor.

3.4. 4MSTB-3MPMI-VBC-DVB networks

4-Methylstilbene (4MSTB) and *N*-(3-methylphenyl)maleimide (3MPMI) were chosen because methyl groups were necessary to ensure the solubility of monomers in the oil phase of the suspension polymerization. The 4MSTB-3MPMI-VBC-DVB hypercrosslinked polymer networks were synthesized via the free radical suspension polymerization followed by Friedle-Crafts post-crosslinking reaction (Scheme 3-1).

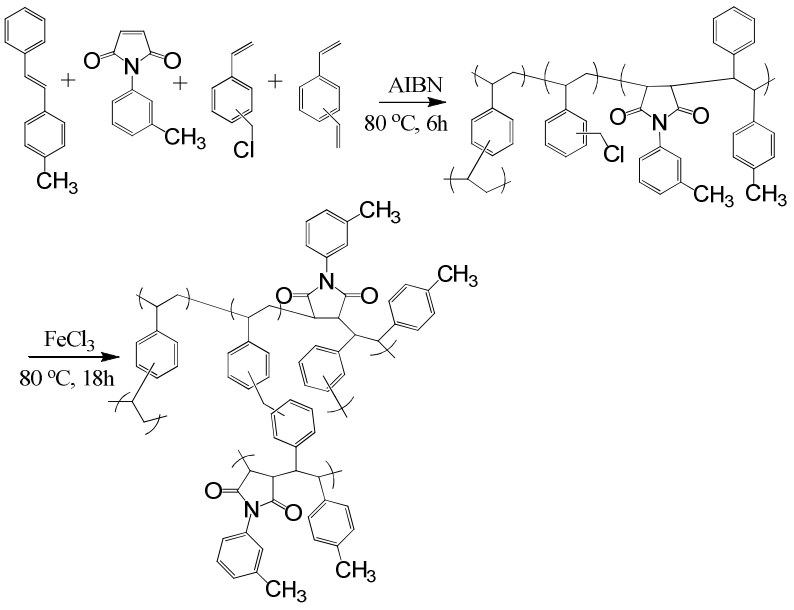

Scheme 3-1. Synthesis scheme for hypercrosslinked poly(4MSTB-3MPMI-VBC-DVB) networks

3.3.1. Thermal Analysis

TGA and DSC were used in order to probe the effect of incorporation of the chain stiffening 4MSTB-3MPMI dyads on the thermal properties of the lightly crosslinked precursor particles from suspension polymerization and hypercrosslinked polymer particles. TGA and DSC curves were shown as follows (Figure 3-3 – 3-12). Table 3-3

summarizes TGA and DSC data.

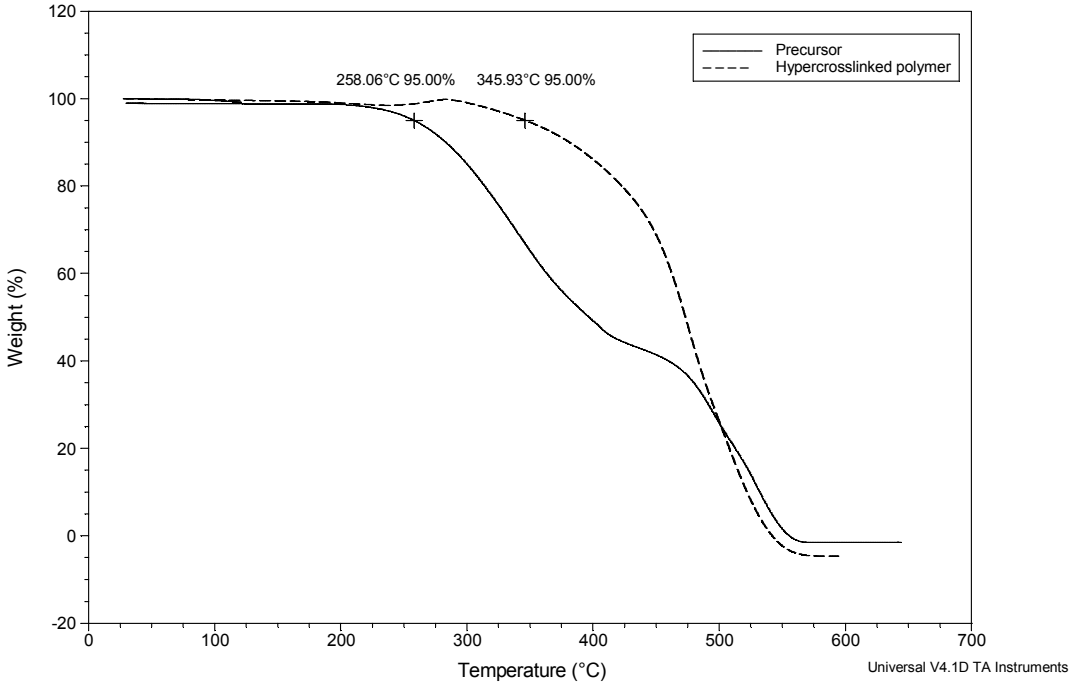

Figure 3-3 TGA curve of (VBC)98(DVB)2

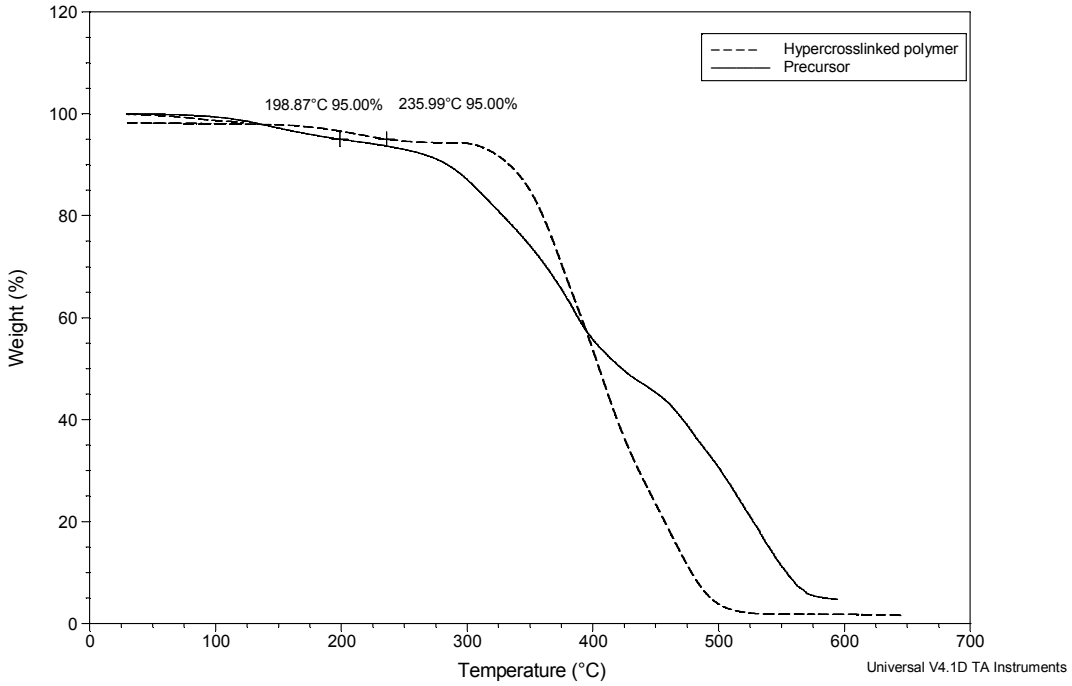

Figure 3-4 TGA curve of (4MSTB-3MPMI)1.0(VBC)98.5(DVB).50

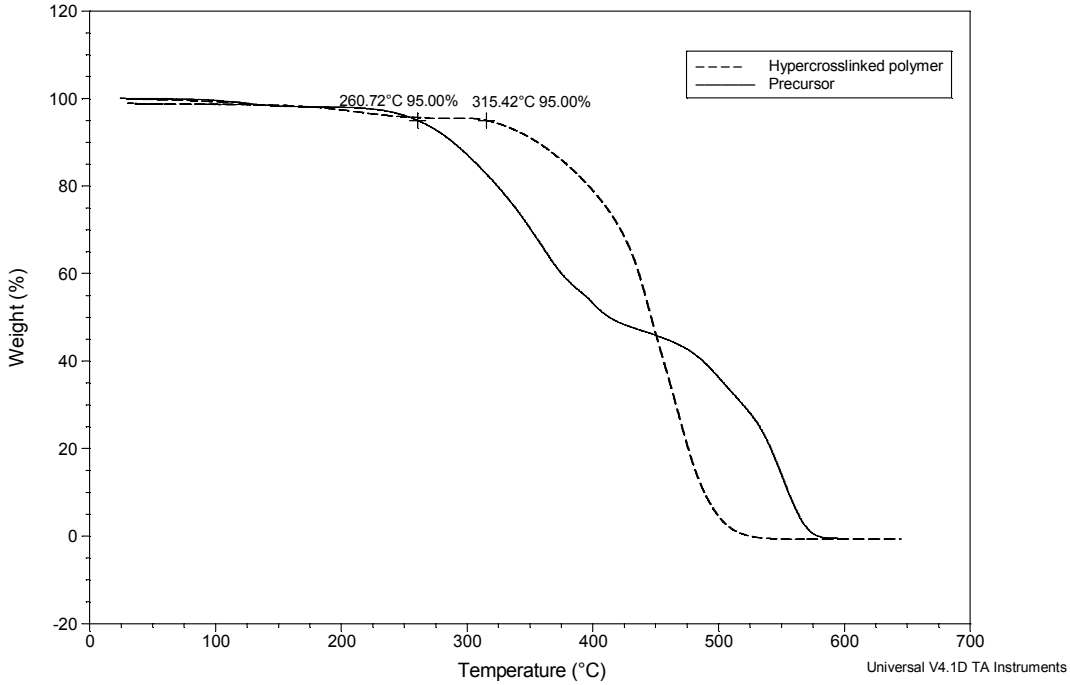

Figure 3-5 TGA curve of (4MSTB-3MPMI)1.9(VBC)97.1(DVB).97

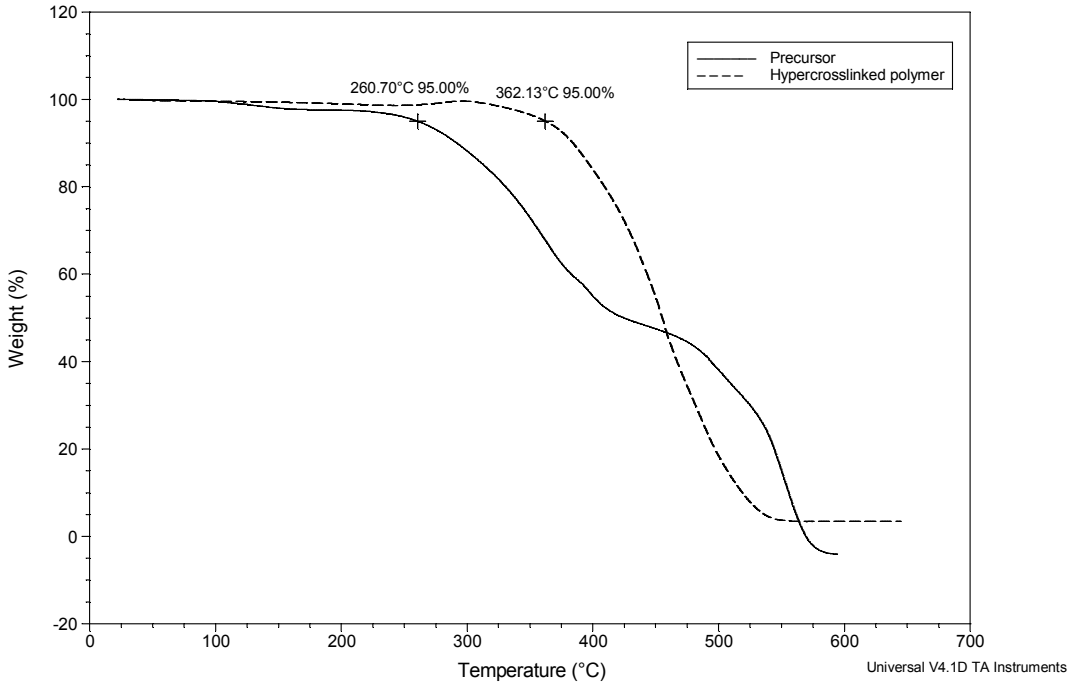

Figure 3-6 TGA curve of (4MSTB-3MPMI)8.7(VBC)87(DVB)4.3

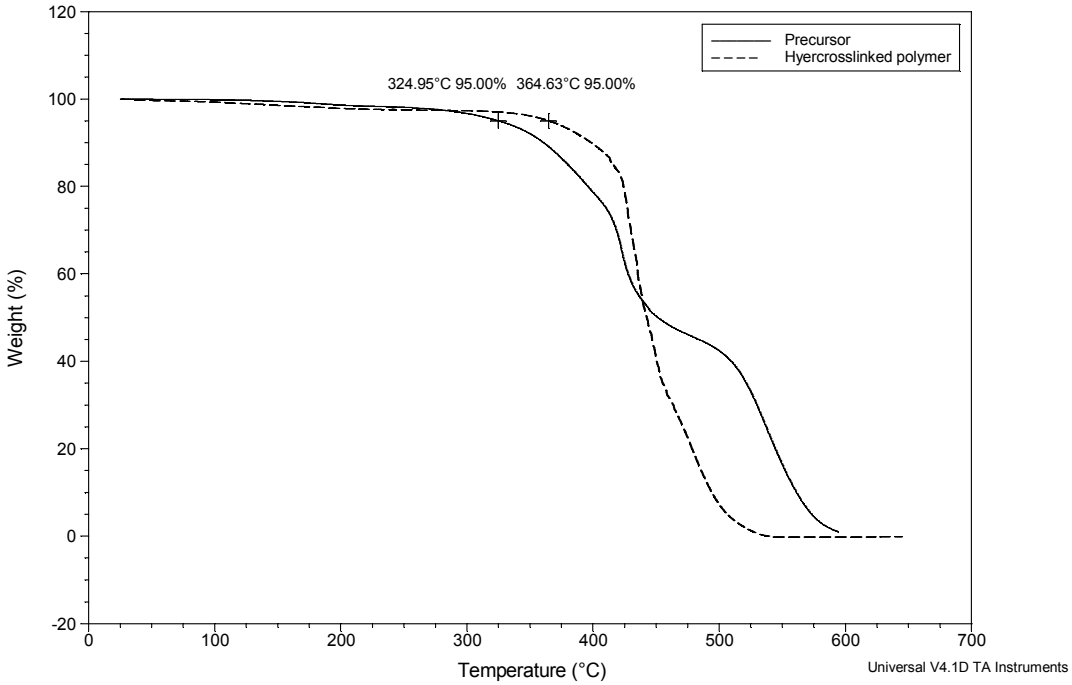

Figure 3-7 TGA curve of (4MSTB-3MPMI)40(VBC)40(DVB)20

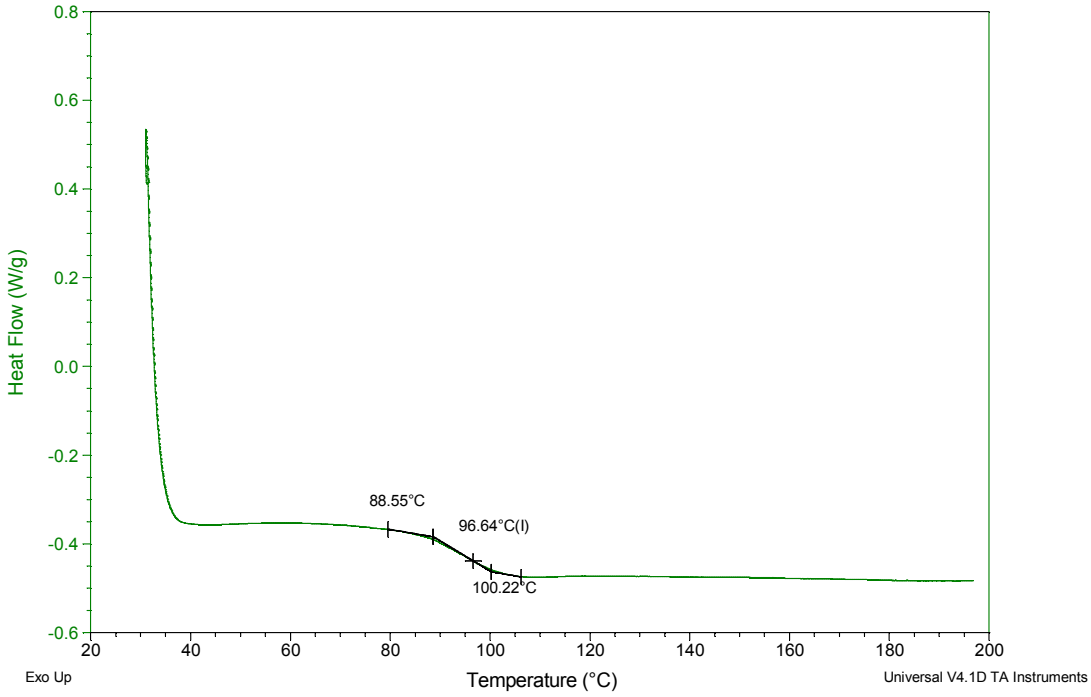

Figure 3-8 DSC curve of (VBC)98(DVB)2 – precursor

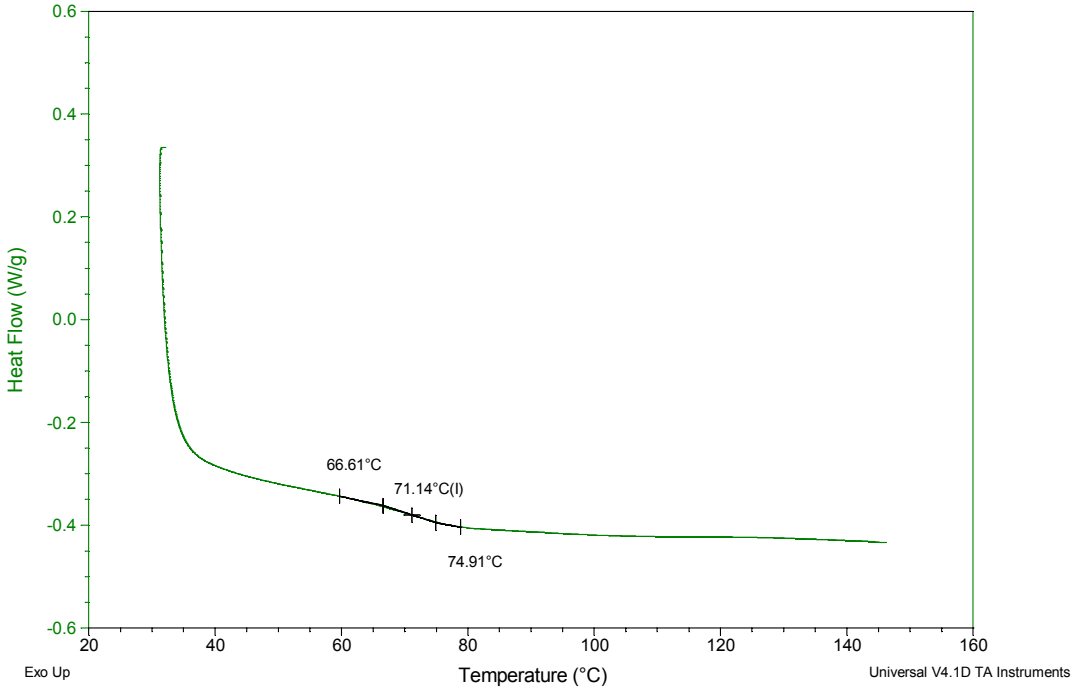

Figure 3-9 DSC curve of (4MSTB-3MPMI)1.0(VBC)98.5(DVB).50 – precursor

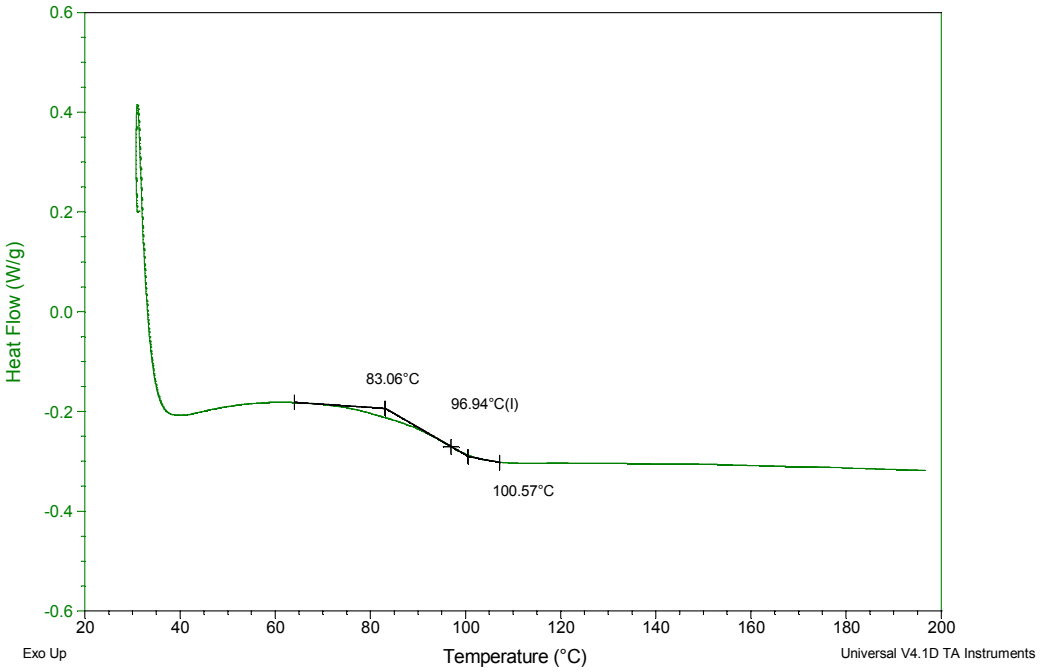

Figure 3-10 DSC curve of (4MSTB-3MPMI)1.9(VBC)97.1(DVB).97 – precursor

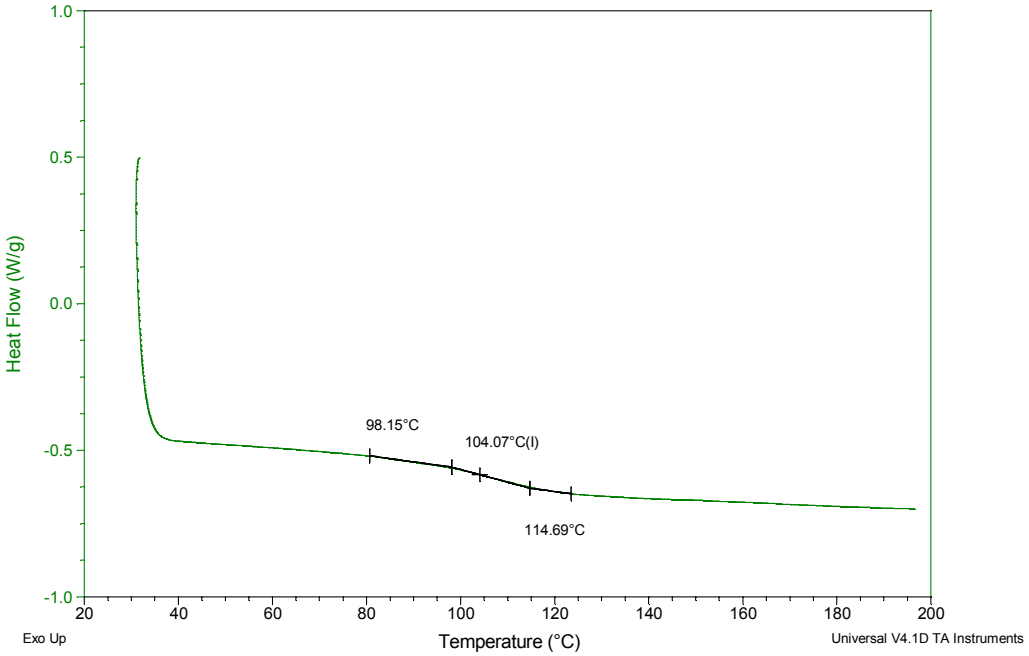

Figure 3-11 DSC curve of (4MSTB-3MPMI)8.7(VBC)87(DVB)4.3 – precursor

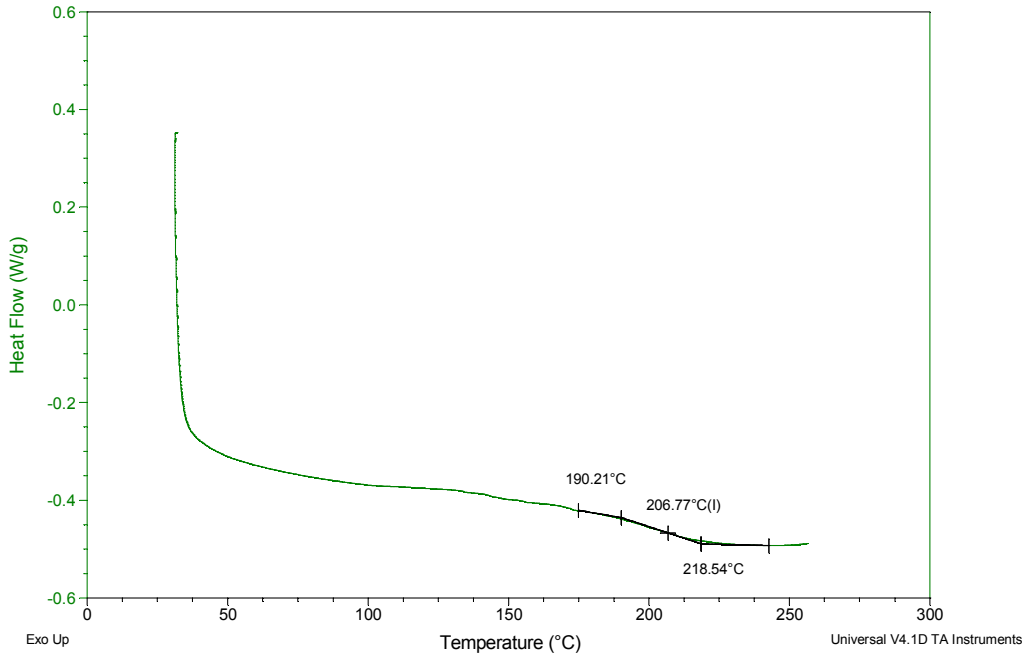

Figure 3-12 DSC curve of (4MSTB-3MPMI)40(VBC)40(DVB)20 – precursor

Table 3-3 Summary of thermal properties of precursors and hypercrosslinked polymers

Name	Precursor		HCL polymer
	T_d, ^oC	T_g, ^oC	T_d, ^oC
(VBC)98(DVB)2	258	96	346
(4MSTB-3MPMI)1.0(VBC)98.5(DVB).50	199	71	236
(4MSTB-3MPMI)1.9(VBC)97.1(DVB).97	261	97	315
(4MSTB-3MPMI)8.7(VBC)87(DVB)4.3	261	104	362
(4MSTB-3MPMI)40(VBC)40(DVB)20	325	207	365

*T_d is the temperature at 5% weight loss.

*For hypercrosslinked polymers, no T_g was observed

Hypercrosslinked polymers have higher thermal stabilities than their lightly crosslinked precursors. From Table 3-3 we can see, all hypercrosslinked polymers have higher decomposition temperature (T_d) than their precursors. No glass transition temperature (T_g) were observed in any of the hypercrosslinked polymers while T_gs from 71^{o}C to 207 ^{o}C were observed in the respective precursors. These observations are consistent with the expected high crosslinked density where there is little segment motions in the hypercrosslinked materials.

For the 4MSTB-3MPMI-VBC-DVB polymer precursor, T_gs increase from 71 ^{o}C to 207 ^{o}C as the mole percentage of 4MSTB-3MPMI segment increases. This is consistent with an increase in the rigidity of polymer backbone with incorporation of 4MSTB-3MPMI segments. However, the T_g of (4MSTB-3MPMI)1.0(VBC)98.5(DVB).50 precursor is 25 ^{o}C lower than that of (VBC)98(DVB)2 precursor. This is probably because of the lower DVB level in

(4MSTB-3MPMI)1.0(VBC)98.5(DVB).50 precursor which causes less crosslinking and more flexibility.

The T_ds of precursor particles and hypercrosslinked polymer increased from 199 ^oC to 325 ^oC and from 236 ^oC to 365 ^oC respectively as mole percentage of 4MSTB-3MPMI segments was increased. These data indicate that incorporation of 4MSTB-3MPMI units enhances the thermal stability of not only precursors but also their respective hypercrosslinked polymers.

The precursor of (4MSTB-3MPMI)1.0(VBC)98.5(DVB).50 has both lower T_d and T_g than the precursor of (VBC)98(DVB)2. Similar trends can be observed in their corresponding hypercrosslinked polymers possibly because of limited amounts of DVB in the (4MSTB-3MPMI)1.0(VBC)98.5(DVB).50 network. (4MSTB-3MPMI)1.0(VBC)98.5(DVB).50 network consists of only 0.5 % DVB which is 25% of the amount of DVB present in (VBC)98(DVB)2. This experiment indicates that the DVB concentration is an important factor needed to achieve thermal properties in the particles.

3.3.2. Pore Structure Study

Scanning electron micrographs (SEM) of both polymer precursors and their respective hypercrosslinked polymers were obtained (Figure 3-13 – 3-22). Most precursors are spherical polymer beads whose size ranges from 50 μm to 200 μm and are consistent with the typical spherical structure yielded from suspension polymerization.

Precursor particles of (4MSTB-3MPMI)1.0(VBC)98.5(DVB).50 (Figure 3-14), (4MSTB-3MPMI)8.7(VBC)87(DVB)4.3 (Figure 3-19), and

(4MSTB-3MPMI)40(VBC)40(DVB)20 (Figure 3-21) were observed to have porous components. Porous structures were observed for all 4MSTB-3MPMI-VBC-DVB hypercrosslinked polymers.

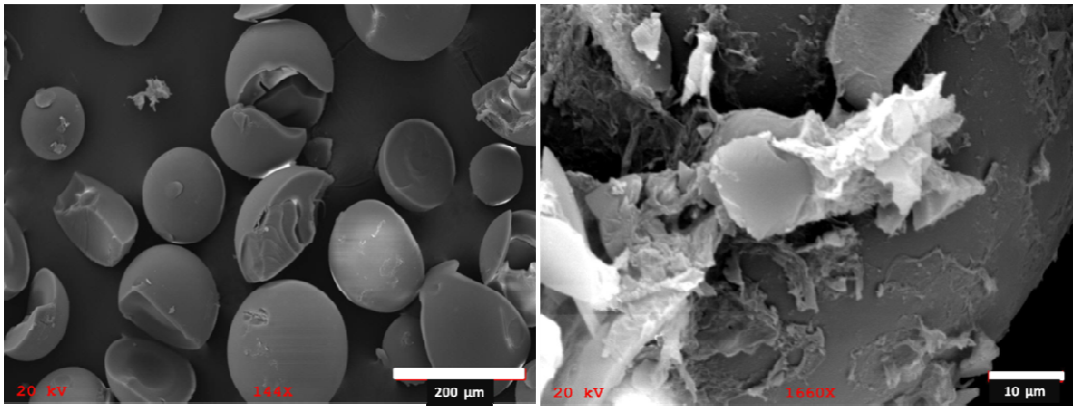

Figure 3-13. SEM of (VBC)98(DVB)2

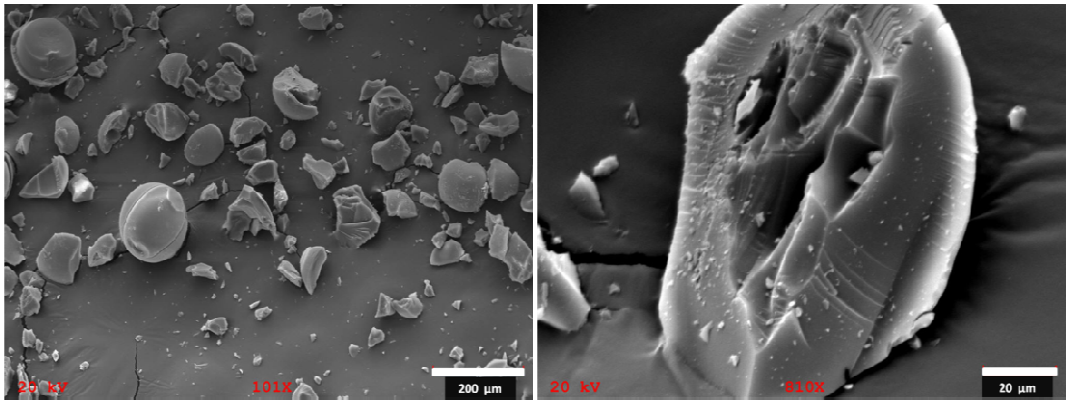

Figure 3-14. SEM of crushed hypercrosslinked (VBC)98(DVB)2

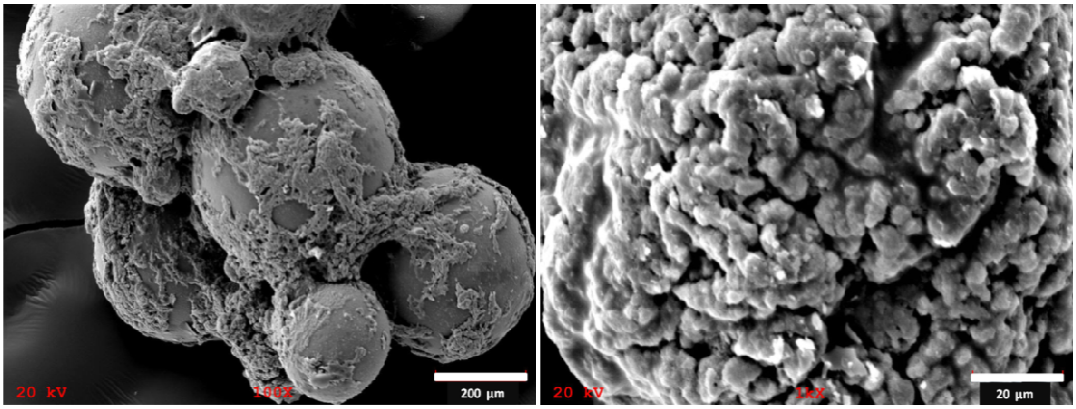

Figure 3-15. SEM of (4MSTB-3MPMI)1.0(VBC)98.5(DVB).50-precursor

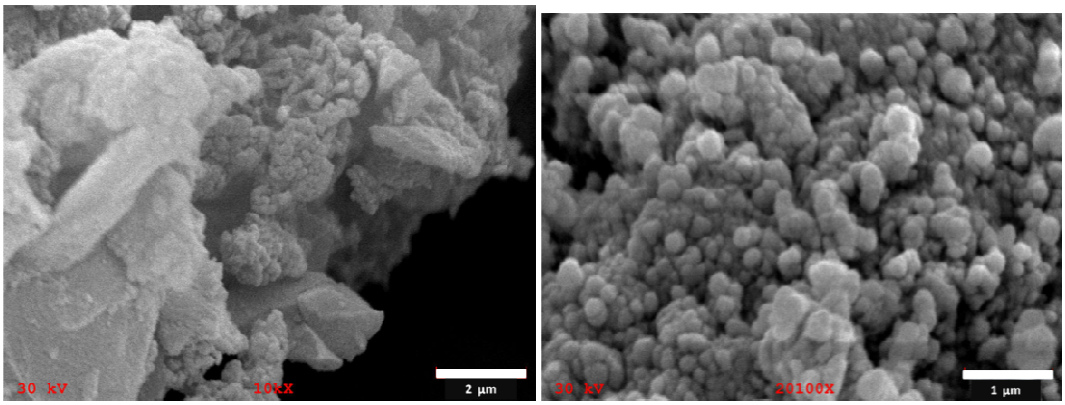

Figure 3-16. SEM of hypercrosslinked (4MSTB-3MPMI)1.0(VBC)98.5(DVB).50

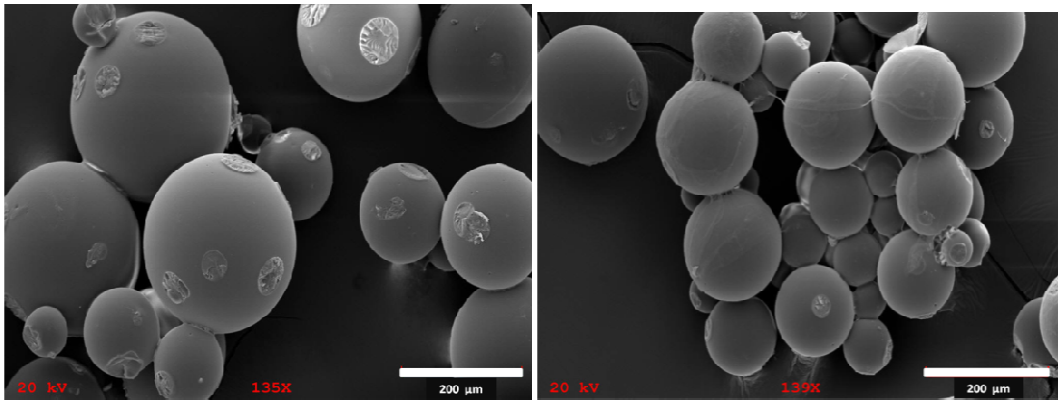

Figure 3-17. SEM of (4MSTB-3MPMI)1.9(VBC)97.1(DVB).97-precursor

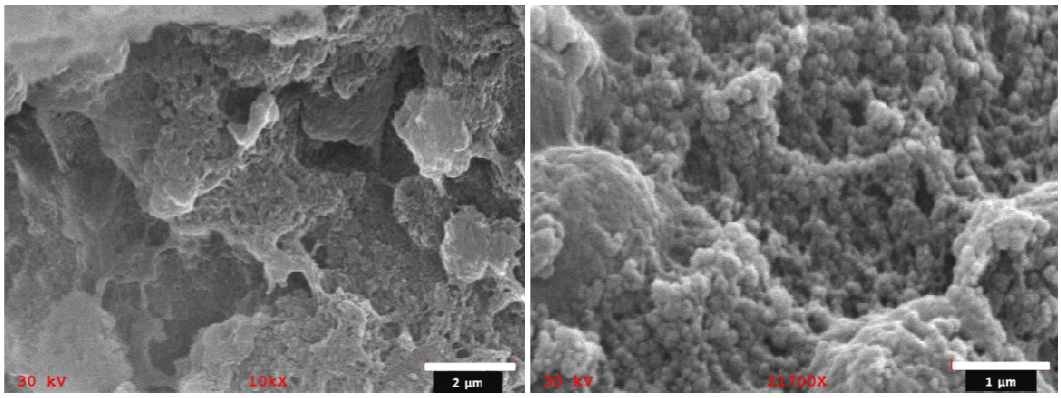

Figure 3-18. SEM of hypercrosslinked (4MSTB-3MPMI)1.9(VBC)97.1(DVB).97

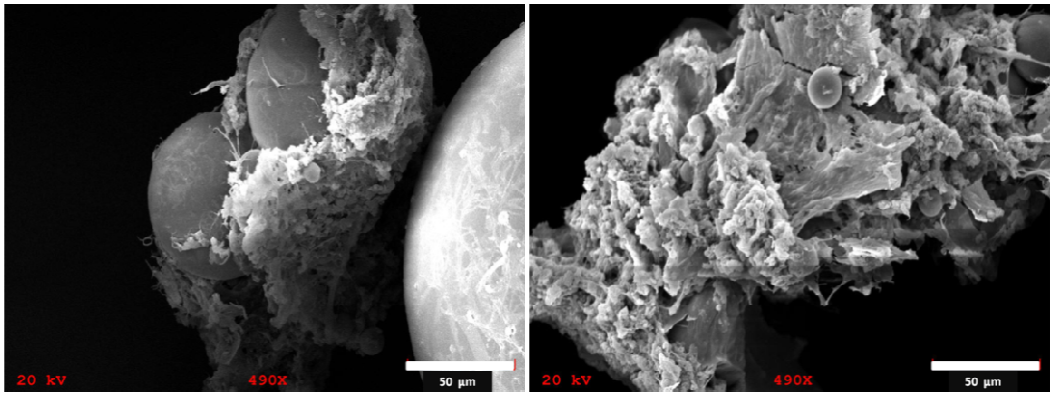

Figure 3-19. SEM of (4MSTB-3MPMI)8.7(VBC)87(DVB)4.3-precursor

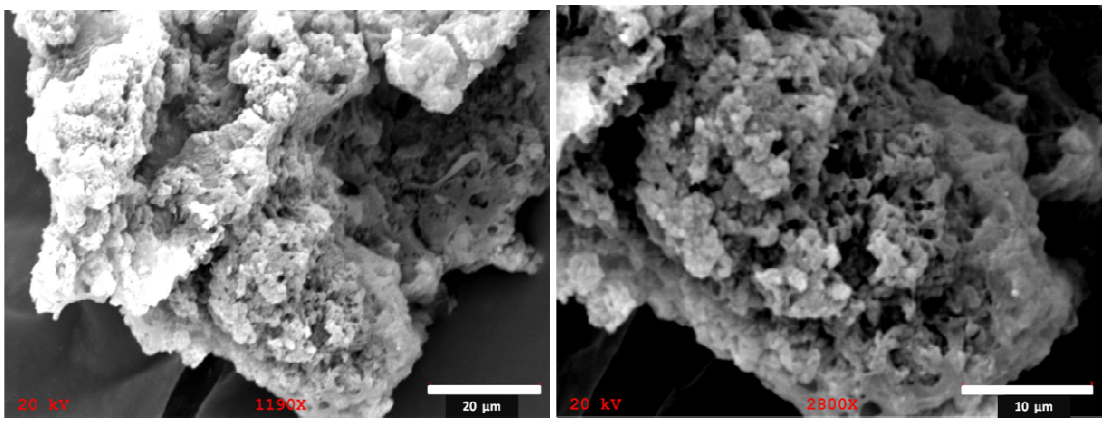

Figure 3-20. SEM of hypercrosslinked (4MSTB-3MPMI)8.7(VBC)87(DVB)4.3

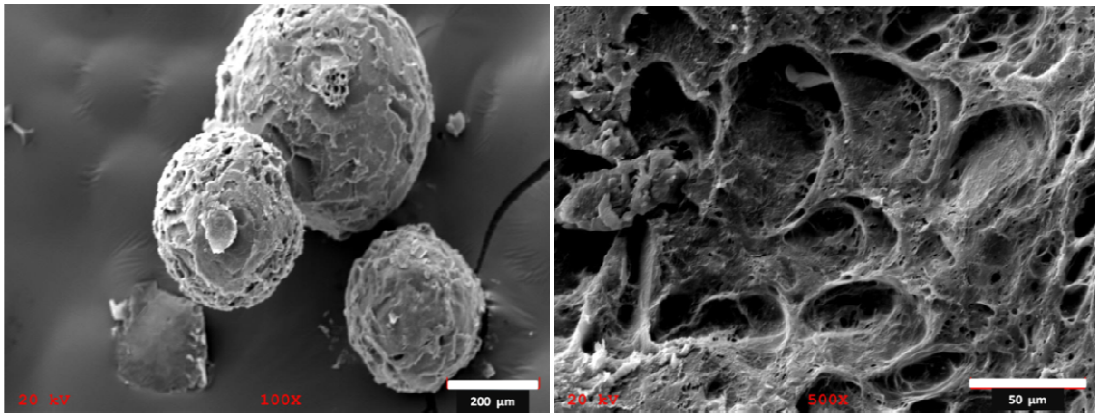

Figure 3-21. SEM of (4MSTB-3MPMI)40(VBC)40(DVB)20-precursor

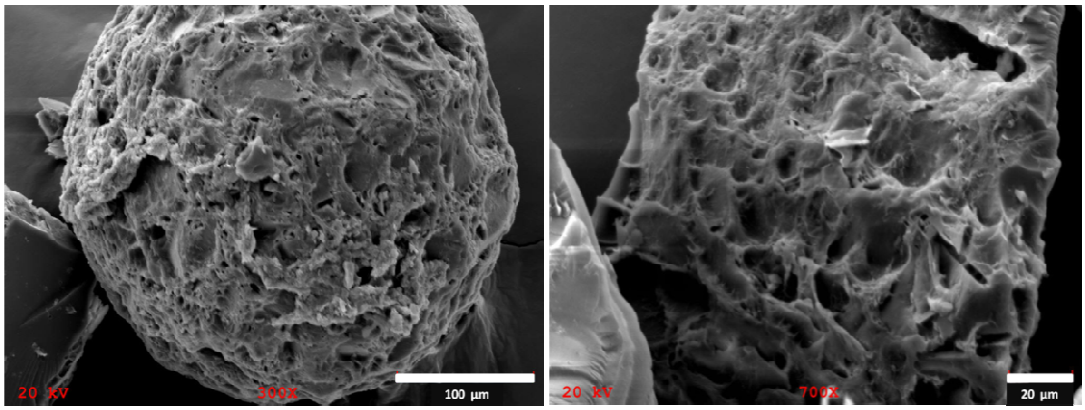

Figure 3-22. SEM of Hypercrosslinked- (4MSTB-3MPMI)40(VBC)40(DVB)20

3.3.3. Surface area study

For porous materials, surface area is an important parameter indicating adsorption sites.[3] Wood et al. synthesized a series of hypercrosslinked polymers and studied the correlation between surface area and hydrogen uptake (Figure 3-23).[37] These results confirm that materials with higher BET surface area generally have higher hydrogen storage capacity.

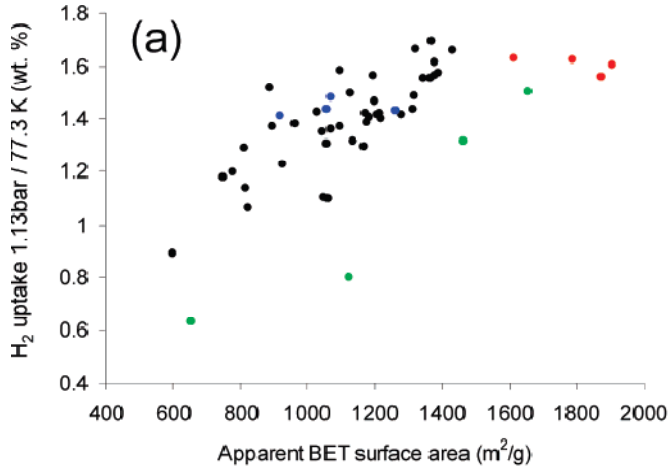

Figure 3-23. Hydrogen uptake at 1.13 bar/77.3 K as a function of apparent BET surface area for a series of hypercrosslinked polymers.[37]

Table 3-4. BET surface area of hypercrosslinked polymers

Name	BET surface area, m^2/g
(VBC)98(DVB)2	1157
(4MSTB-3MPMI)1.0(VBC)98.5(DVB).50	1092
(4MSTB-3MPMI)1.9(VBC)97.1(DVB).97	1106
(4MSTB-3MPMI)8.7(VBC)87(DVB)4.3	-
(4MSTB-3MPMI)40(VBC)40(DVB)20	284

BET surface area results of hypercrosslinked polymers are shown in Table 3-4. (VBC)98(DVB)2 is used as control, (4MSTB-3MPMI)1.0(VBC)98.5(DVB).50 and (4MSTB-3MPMI)1.9(VBC)97.1(DVB).97 have similar surface area when compared to (VBC)98(DVB)2. (4MSTB-3MPMI)40(VBC)40(DVB)20 exhibited low surface area of only 284 m^2/g. This may due to the dilution of VBC when too much 4MSTB-3MPMI was incorporated because the chloromethyl group in VBC is the crosslinker in the hypercrosslinking step.

3.5. Styrene (STR)-VBC-DVB networks

In order to further investigate the effect of chloromethyl group on surface area of hypercrosslinked network, a series of hypercrosslinked STR-VBC-DVB networks were synthesized with various amounts of VBC while keeping the amount of DVB constant (Scheme 3-2). SEM micrographs of hypercrosslinked STR-VBC-DVB particles were taken and pore structures were observed in all particles (Figure 3-24 – 3-25).

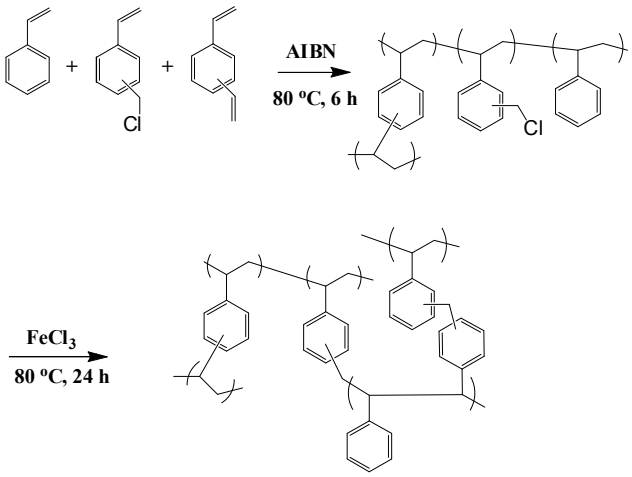

Scheme 3-2. Synthesis scheme of hypercrosslinked STR-VBC-DVB polymer networks

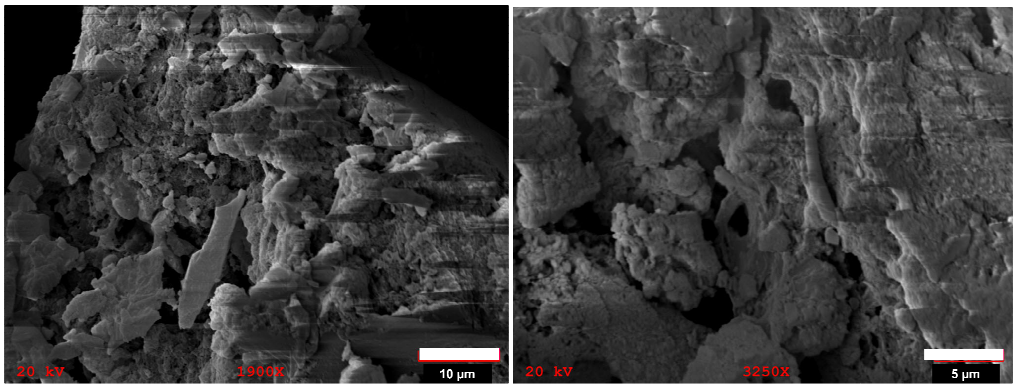

Figure 3-24. SEM of hypercrosslinked (STR)24.5(VBC)73.5(DVB)2 (left) and hypercrosslinked (STR)49 (VBC)49 (DVB)2 (right)

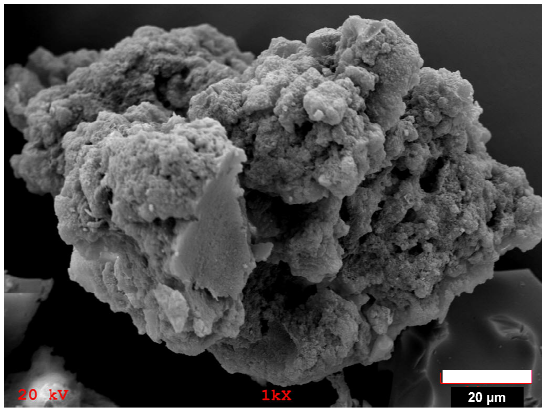

Figure 3-25. SEM of hypercrosslinked (STR)73.5(VBC)24.5(DVB)2

BET surface areas were measured and shown in Table 3-5 along with the thermal properties. A systematic decrease in BET surface area from 2822 to 935 m^2/g was observed when the mole percentage of VBC decreases from 73.5% to 24.5%. The plot of BET surface area verses mole percentage of VBC shows the liner correlation between these two components (Figure 3-26). Therefore, maintaining a high density of chloromethyl groups is crucial in order to achieve high surface area.

Table 3-5. BET surface area data and thermal properties of STR-VBC-DVB polymer networks

Name	Precursor		Hypercrosslinked polymer	
	T_d, ℃	T_g, ℃	T_d, ℃	BET surface area, m^2/g
(STR)24.5(VBC)73.5(DVB)2	252	93	332	2822
(STR)49 (VBC)49 (DVB)2	276	103	303	1937
(STR)73.5(VBC)24.5(DVB)2	285	105	326	935

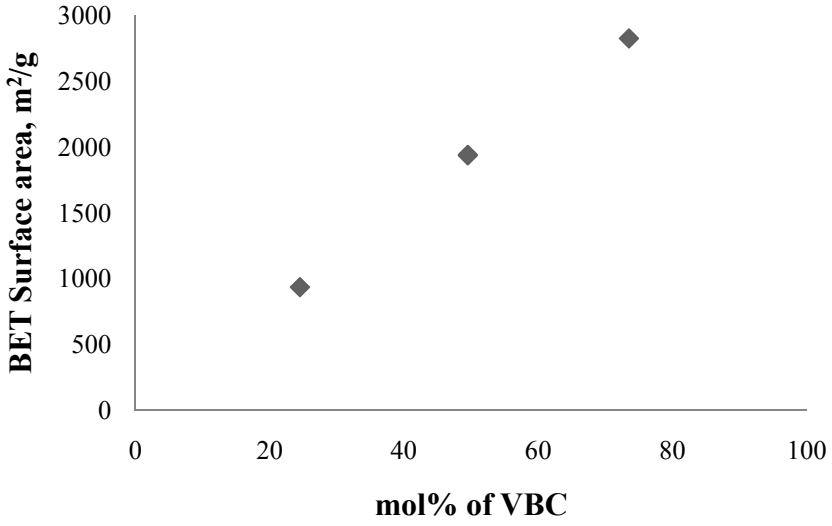

Figure 3-26. BET surface area as a function of mole percent of VBC

3.6. 4MSTB-3MPMI-VBC-N-allylmaleimide(AMI) network

N-Allylmaleimide was used to replace divinylbenzene which served as a crosslinker in suspension polymerization to form lightly crosslinking precursor. Hypercrosslinked polymer (4MSTB-3MPMI)1.9(VBC)97.1(AMI).97 was synthesized using the same synthetic scheme as hypercrosslinked polymer network previously synthesized (Scheme 3-3). Porous structures were observed in both precursor particles and hypercrosslinked polymers from SEM micrographs (Figure 3-27 – 3-28).

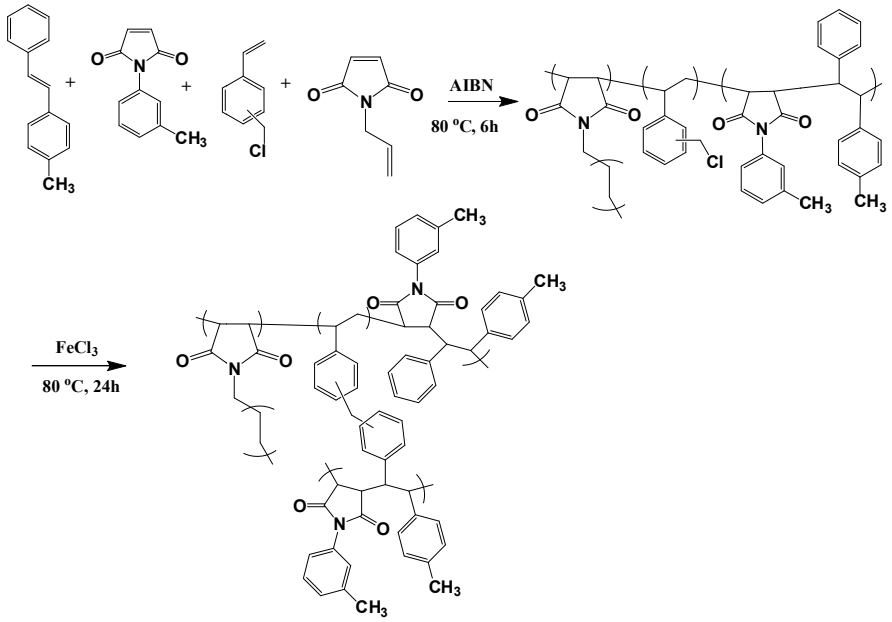

Scheme 3-3. Synthesis of hypercrosslinked 4MSTB-3MPMI-VBC-AMI network

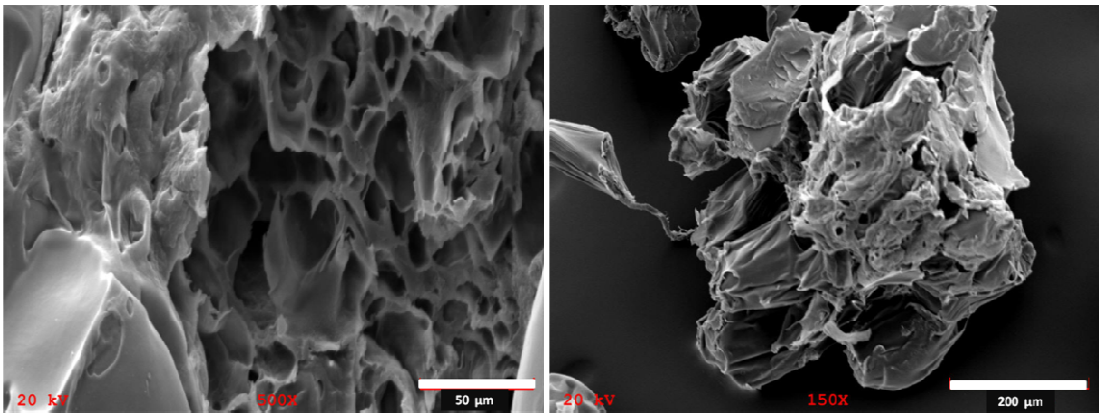

Figure 3-27. SEM of (4MSTB-3MPMI)1.9(VBC)97.1(AMI).97-precursor

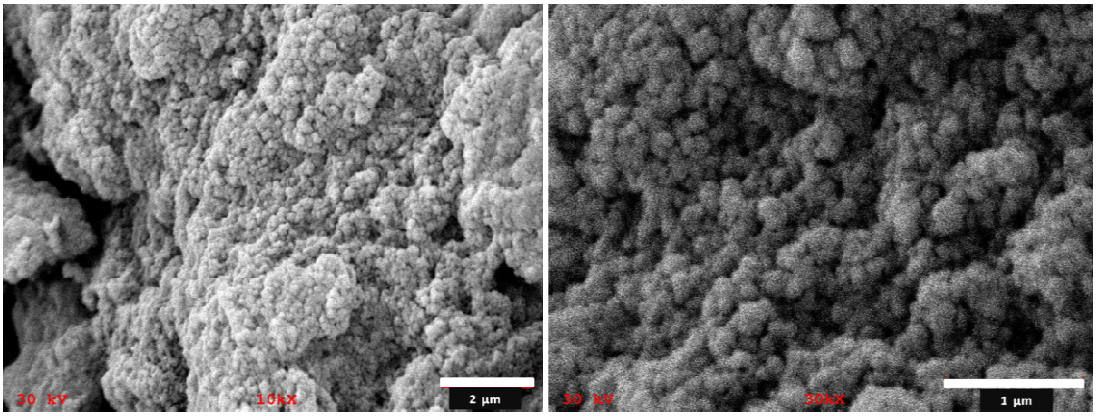

Figure 3-28. SEM of hypercrosslinked (4MSTB-3MPMI)1.9(VBC)97.1(AMI).97

Thermal properties and BET surface area data of both precursor and hypercrosslinked polymer were measured and compared with (VBC)98(DVB)2 and 4MSTB-3MPMI-VBC-DVB network (Table 3-6). TGA and DSC curves were shown in Figure 3-29 and 3-30.

These results indicate, that at this low level, incorporation of the same amount of AMI instead of DVB results in particles with similar thermal properties. The BET surface did not change much by replacing DVB with AMI, from 1106 to 1153 m^2/g. Therefore, AMI could potentially serve as a crosslinker to replace DVB without compromising surface area.

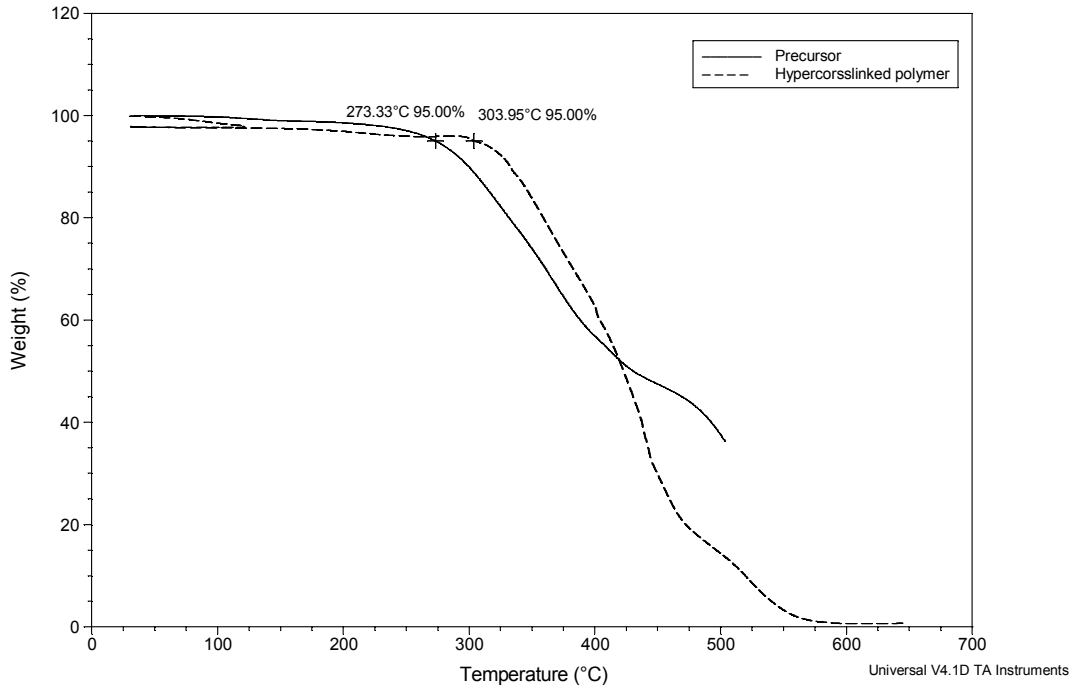

Figure 3-29. TGA curve of (4MSTB-3MPMI)1.9(VBC)97.1(AMI).97

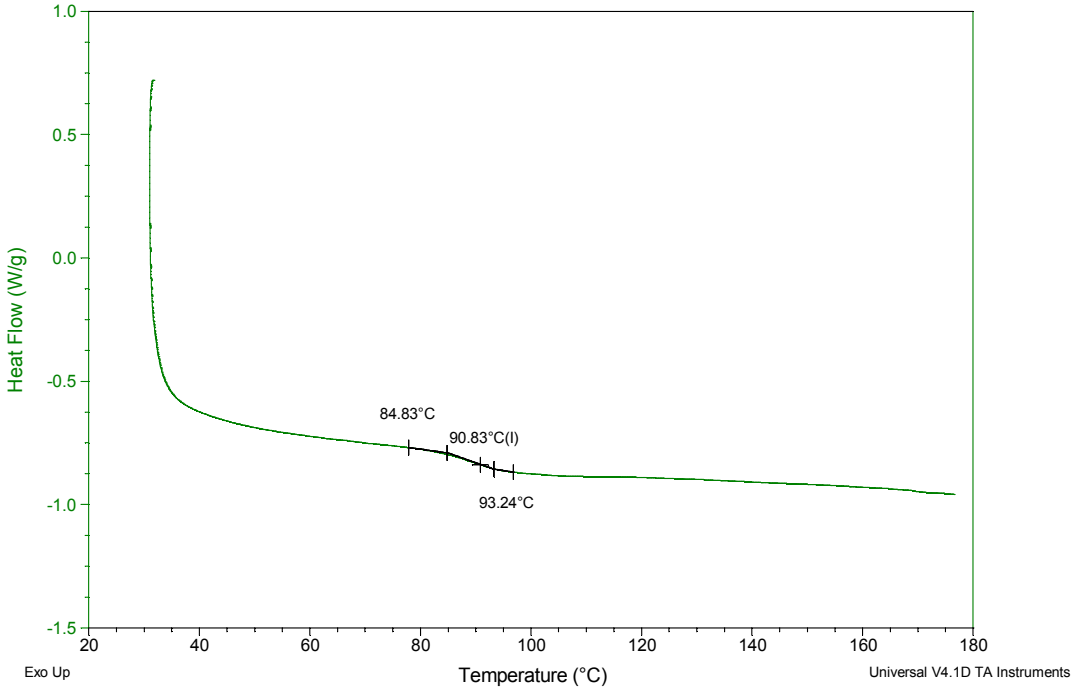

Figure 3-30. DSC curve of (4MSTB-3MPMI)1.9(VBC)97.1(AMI).97 – precursor

Table 3-6. Thermal properties and BET surface area of (4MSTB-3MPMI)1.9(VBC)97.1(AMI).97 polymer network comparing with (VBC)98(DVB)2 and 4MSTB-3MPMI-VBC-DVB networks

Name	Precursor		HCL polymer	
	T_d,℃	T_g,℃	T_d,℃	BET surface area,m^2/g
(VBC)98(DVB)2	258	96	258	1157
(4MSTB-3MPMI)1.9(VBC)97.1(DVB).97	261	97	315	1106
(4MSTB-3MPMI)1.9(VBC)97.1(AMI).97	273	91	304	1153

3.7. 4CMSTB-3CMPMI-DVB network

As discussed earlier study, incorporation of a functionalized stilbene – N-substituted maleimide segments increases the rigidity of polymer backbone with evidence of increasing T_gs of the precursor particles. However, our systematic study of the styrene control system clearly shows that reduction in the chloromethyl group level leads to lower surface areas. Therefore, incorporation of significant levels of the stilbene - maleimide alternating copolymer into the particles requires that these monomers contain chloromethyl groups. For this reason monomer 4CMSTB and 3CMPMI were synthesized. Scheme 3-4 shows the hypercrosslinking reactions for these functionalized copolymers. The SEM micrograph of (4CMSTB)49(3CMPMI)49(DVB)2 shows porous structure (Figure 3-31). However, BET surface data is pending.

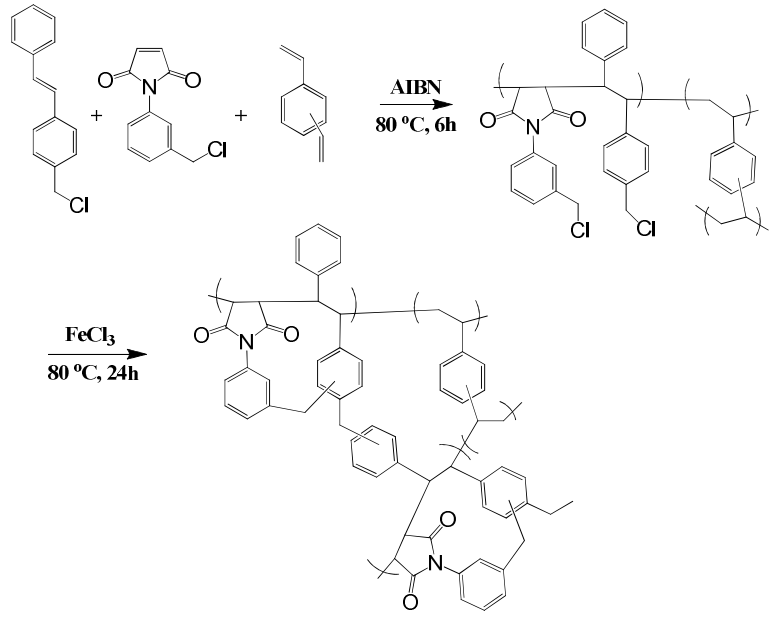

Scheme 3-4. Synthesis of hypercrosslinked 4CMSTB-3CMPMI-DVB network

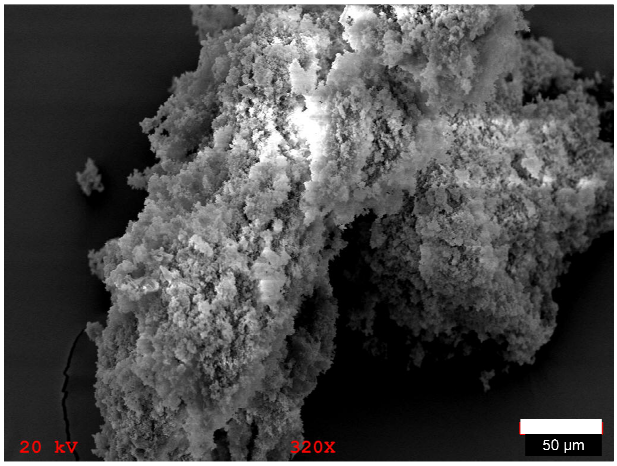

Figure 3-31. SEM of hypercrosslinked (4CMSTB)49(3CMPMI)49(DVB)2

3.8. 4,4'DASTB-3MPMI-DVB network

Hydrogen adsorption enthalpy determines the temperature at which reversible hydrogen storing occurs and the suggested value at room temperature is 15 kJ/mol.[3] However, recent nanostructure materials have enthalpy of hydrogen adsorption of 4-7 kJ/mol resulting in the necessary of applying low temperature (77K) for achieving maximum uptake. Hypercrosslinked polyanilines synthesized by Svec et al. exihibited enthalpy of hydrogen adsorption up to 7.9 kJ/mol which make hydrogen storage at room temperature more feasible.[2] These data confirm that the incorporation of electron donating groups increases the enthalpy of hydrogen adsorption in polymeric materials.[2] Therefore, based on these results the monomer N,N-dimethyl-N',N'-diethyl-4,4'-diaminostilbene (4,4'DASTB) which contains electron donating groups was chosen to incorporate into hypercrosslinked polymer network (Scheme 3-5). Therefore, hypercrosslinked (4,4' DASTB-3MPMI)1.0(VBC)98.5(DVB).50 was synthesized. The porous structure was observed in hypercrosslinked polymer particles (Figure 3-32). The T_g of (4,4'

DASTB-3MPMI)1.0(VBC)98.5(DVB).50 precursor is 80.0 ^{o}C (Figure 3-33).

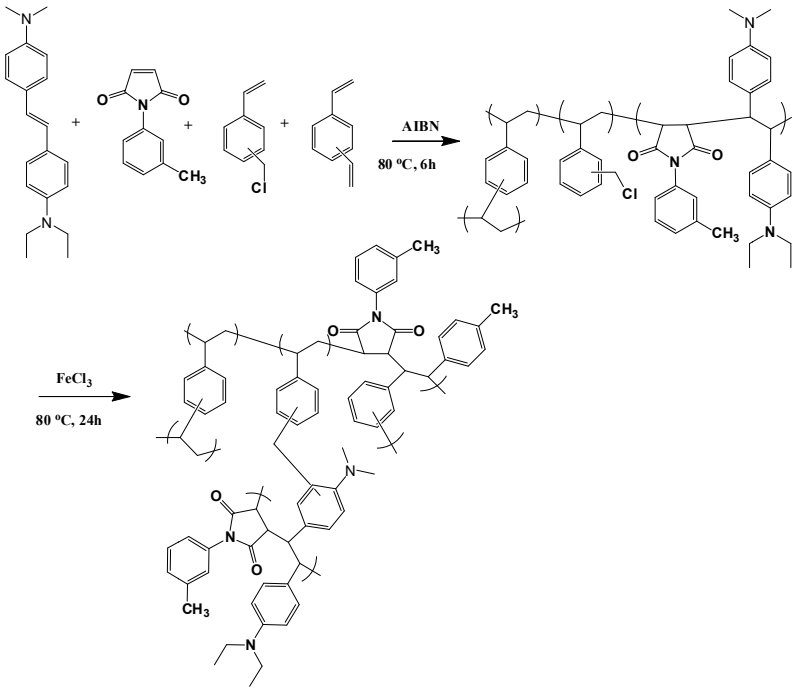

Scheme 3-5. Synthesis of hypercrosslinked 4,4' DASTB-3MPMI-DVB network

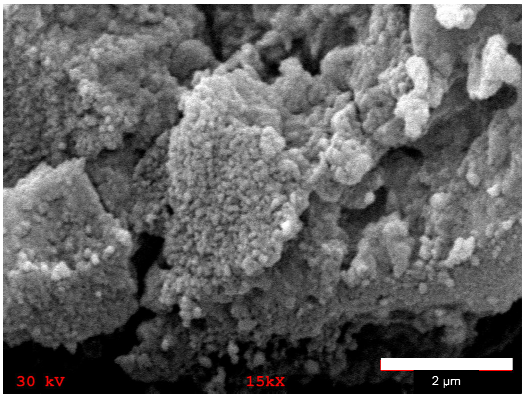

Figure 3-32. SEM of hypercrosslinked (4,4'

DASTB-3MPMI)1.0(VBC)98.5(DVB).50

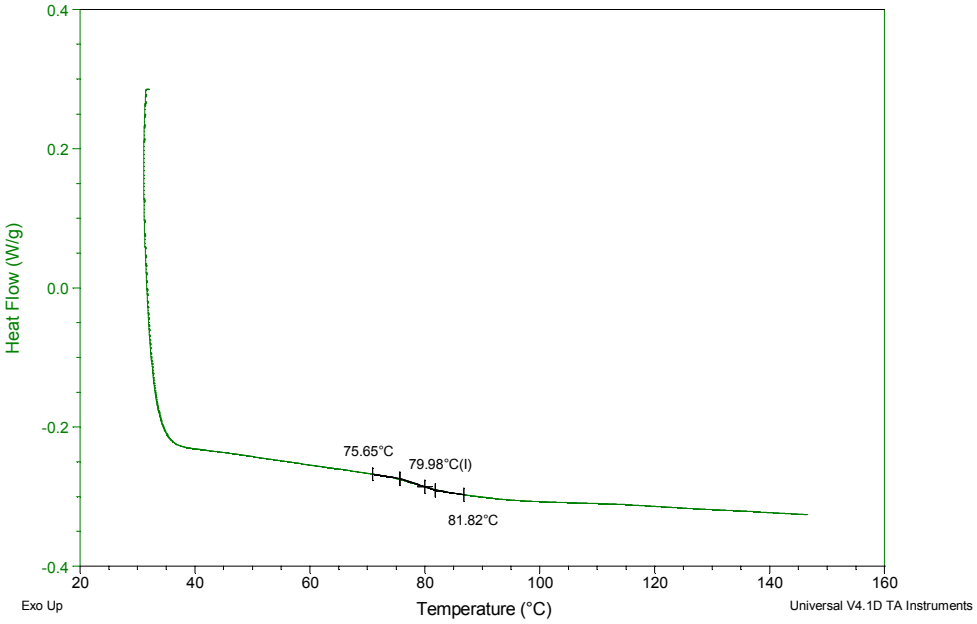

Figure 3-33. DSC curve of (4,4' DASTB-3MPMI)1.0(VBC)98.5(DVB).50 - precursor

The BET surface area of hypercrosslinked (4,4 ' DASTB-3MPMI)1.0(VBC)98.5(DVB).50 is 3257 m^2/g, which is the highest one among all hypercrosslinked polymers we synthesized so far. In a previous study in our group, amino group containing stilbene-maleic anhydride alternating copolymers formed predominately *cis* configuration of H-C-C-H of the anhydride ring from the solid state NMR results.[68] This cis configuration may cause the polymer chains to become contorted and thus pack inefficiently to yield internal free volume (Figure 3-34). Although maleimide monomers are not as electron poor as maleic anhydride, a similar configuration might form in 4,4'DASTB-3MPMI-DVB networks which could give more free volume and thus have higher surface area.

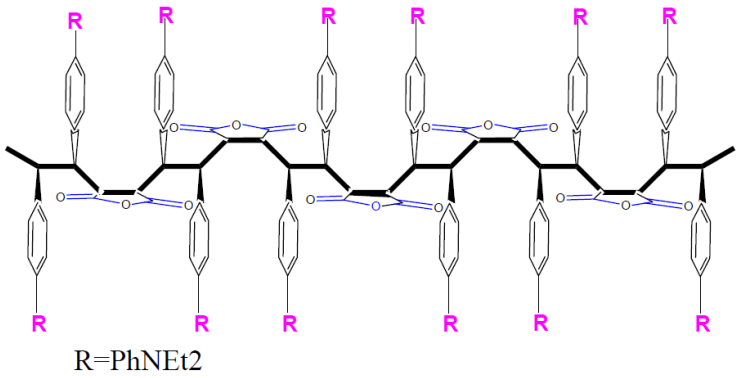

Figure 3-34. Possible chain configuration of the functional groups of TDAS-MA alternating copolymer[68]

3.9. Conclusions

In our study, functionalized stilbene and N-substituted maleimide monomers were successfully synthesized. Hypercrosslinked polymers containing functionalized stilbene and N-substituted maleimide were synthesized as well. The carbonyl stretching band around 1700 cm^{-1} from infrared spectroscopy confirmed the incorporation of N-substituted maleimide. Spherical particles from precursors and porous structures from hypercrosslinked polymers were observed in SEM micrograph.

Incorporation of the 4MSTB-3MPMI segment enhanced the rigidity of the polymer backbone and thermal stability. However, dilution of chloromethyl group caused a decrease in BET surface area. Therefore, a functionalized stilbene-N-substituted maleimide containing chloromethyl groups was utilized in order to enhance rigidity of the polymer backbone without compromising BET surface area. The AMI monomer can serve as a crosslinker in the suspension polymerization to replace DVB and form a hypercrosslinked polymer with similar BET surface area. A high BET surface area of

3257 m^2/g was achieved from the amino group containing hypercrosslinked polymer.

3.10. Acknowledgements

We would like to acknowledge the Lawrence Berkeley National Lab for BET surface area measurements. We would also like to acknowledge the National Science Foundation (NSF) under grant number DMR-0905-231 for financial support.

CHAPTER 4. FUTURE WORK

Future research will continue investigating monomers' effect on the properties of hypercrosslinked polymer networks in order to achieve high surface area, high hydrogen storage capacity and higher enthalpy of hydrogen adsorption.

4.1. Hypercrosslinked polymer networks synthesized by chloromethyl containing monomers

Our previous study shows the importance of maintaining a high density of chloromethyl group to keep high surface area. After getting surface area data of hypercrosslinked (4CMSTB)49(3CMPMI)49(DVB)2 polymer, we will optimize the amount of 4CMSTB-3CMPMI segments to get higher surface area. Also, AMI will be used to replace DVB in the polymer network. It is interesting to see how will AMI affect the surface area of hypercrosslinked polymer.

4.2. Hypercrosslinked polymer networks with electron donating groups

The polymer network (4,4'DASTB-3MPMI)1.0(VBC)98.5(DVB).50 which has the highest surface area in our study will be sent to the Lawrence Berkeley National Lab for hydrogen storage measurement. Meanwhile, we will continue to study 4,4'DASTB-3MPMI-VBC-DVB networks to optimize the compositions of monomers to achieve high surface area.

In order to understand the effect of contorted polymer chain on surface area, several

amino containing stilbene – maleic anhydride alternating copolymers were submitted for surface area measurement. The data will be used to compare with surface area data of 4,4'DASTB-3MPMI-VBC-DVB networks and will be compared to the PIM literature.

New stilbene derivatives containing electron donating groups would be excellent targets for systematically varying the electron density of the aromatic group. Examples are shown below (Figure 4-1).

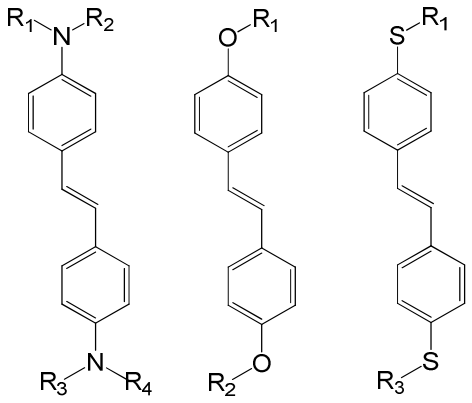

Figure 4-1. Stilbene derivatives containing electron donating groups

3MPMI will be replaced by chloromethyl group - containing maleimide such as 3CMPMI to further increase crosslinking density and thus increase surface area. Moreover, the enthalpy of hydrogen adsorption might be studied. An increase in enthalpy with electron donating group containing polymer is expected.

4.3. Hypercrosslinked polymer network containing styrylnaphthalene derivatives

It is interesting to incorporate styrylnaphthalene derivatives into hypercrosslinked polymer network to increase the density of aromatic groups which are believed to be

major adsorption site without the presence of metal. Moreover, the kinked structure of styrylnaphthalene derivatives might make the polymer chain contorted and thus form internal free volume. An increase in surface area is expected.

1-Styrylnaphthalene (1SNT) will be used and copolymerized with 3MPMI, VBC and DVB (Scheme 4-1). The thermal properties and surface area results will be compared to those from the 4MSTB-3MPMI-VBC-DVB network.

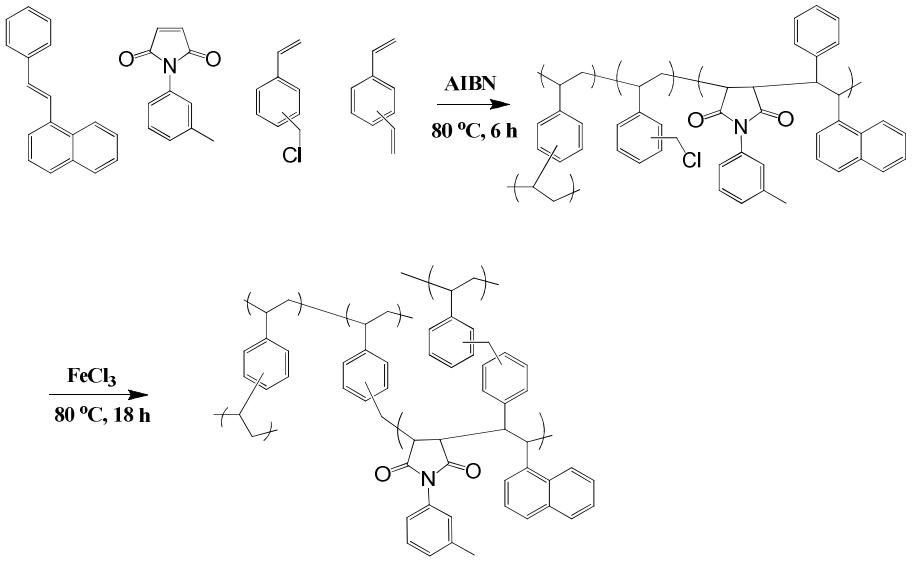

Scheme 4-1. Synthesis of hypercrosslinked 1SNT-3MPMI-VBC-DVB network

References

(1) Germain, J.; Hradil, J.; Frechet, J. M. J.; Svec, F. *Chemistry of Materials* **2006**, *18*, 4430.

(2) Germain, J.; Frechet, J. M. J.; Svec, F. *J Mater Chem* **2007**, *17*, 4989.

(3) Germain, J.; Frechet, J. M. J.; Svec, F. *Small* **2009**, *5*, 1098.

(4) McKeown, N. B.; Budd, P. M. *Chemical Society Reviews* **2006**, *35*, 675.

(5) *Global Carbon Project (2008) Carbon budget and trends 2007*, 2008.

(6) van den Berg, A. W. C.; Arean, C. O. *Chemical Communications (Cambridge, United Kingdom)* **2008**, 668.

(7) Wang, L.; Yang, R. T. *Energy Environ. Sci.* **2008**, *1*, 268.

(8) In *http://www1.eere.energy.gov/hydrogenandfuelcells/storage/current_technology.html*.

(9) Kaye, S. S.; Dailly, A.; Yaghi, O. M.; Long, J. R. *J Am Chem Soc* **2007**, *129*, 14176.

(10) Wong-Foy, A. G.; Matzger, A. J.; Yaghi, O. M. *J Am Chem Soc* **2006**, *128*, 3494.

(11) Furukawa, H.; Miller, M. A.; Yaghi, O. M. *J Mater Chem* **2007**, *17*, 3197.

(12) Ghanem, B. S.; Msayib, K. J.; McKeown, N. B.; Harris, K. D. M.; Pan, Z.; Budd, P. M.; Butler, A.; Selbie, J.; Book, D.; Walton, A. *Chemical Communications (Cambridge, United Kingdom)* **2007**, 67.

(13) Ghanem, B. S.; McKeown, N. B.; Budd, P. M.; Fritsch, D. *Macromolecules (Washington, DC, U. S.)* **2008**, *41*, 1640.

(14) Makhseed, S.; Samuel, J.; Bumajdad, A.; Hassan, M. *J Appl Polym Sci* **2008**, *109*, 2591.

(15) Panella, B.; Hirscher, M.; Roth, S. *Carbon* **2005**, *43*, 2209.

(16) Yang, Z.; Xia, Y.; Mokaya, R. *J Am Chem Soc* **2007**, *129*, 1673.

(17) Pacula, A.; Mokaya, R. *Journal of Physical Chemistry C* **2008**, *112*, 2764.

(18) Germain, J.; Frechet, J. M. J.; Svec, F. *PMSE Preprints* **2007**, *97*, 272.

(19) Lee, J.-Y.; Wood Colin, D.; Bradshaw, D.; Rosseinsky Matthew, J.; Cooper Andrew, I. *Chemical Communications (Cambridge, England)* **2006**, 2670.

(20) Stroebel, R.; Garche, J.; Moseley, P. T.; Joerissen, L.; Wolf, G. *Journal of Power Sources* **2006**, *159*, 781.

(21) Dillon, A. C.; Heben, M. J. *Applied Physics A Materials Science & Processing* **2001**, *72*, 133.

(22) Carpetis, C.; Peschka, W. *International Journal of Hydrogen Energy* **1980**, *5*, 539.

(23) Dresselhaus, M. S.; Dresselhaus, G.; Saito, R. *Carbon* **1995**, *33*, 883.

(24) Rzepka, M.; Lamp, P.; De la Casa-Lillo, M. A. *J Phys Chem B* **1998**, *102*, 10894.

(25) Hou, P.-x.; Yang, Q.-h.; Bai, S.; Xu, S.-t.; Liu, M.; Cheng, H.-m. *J Phys Chem*

B **2002**, *106*, 963.

(26) Han, S. S.; Furukawa, H.; Yaghi, O. M.; Goddard, W. A., III *J Am Chem Soc* **2008**, *130*, 11580.

(27) El-Kaderi, H. M.; Hunt, J. R.; Mendoza-Cortes, J. L.; Cote, A. P.; Taylor, R. E.; O'Keeffe, M.; Yaghi, O. M. *Science (Washington, DC, United States)* **2007**, *316*, 268.

(28) Cote, A. P.; Benin, A. I.; Ockwig, N. W.; O'Keeffe, M.; Matzger, A. J.; Yaghi, O. M. *Science (Washington, DC, United States)* **2005**, *310*, 1166.

(29) Isaeva, V. I.; Kustov, L. M. *Russian Journal of General Chemistry* **2007**, *77*, 721.

(30) Papaefstathiou, G. S.; MacGillivray, L. R. *Coordination Chemistry Reviews* **2003**, *246*, 169.

(31) Sun, D.; Ma, S.; Ke, Y.; Collins, D. J.; Zhou, H.-C. *J Am Chem Soc* **2006**, *128*, 3896.

(32) Yaghi, O. M.; O'Keeffe, M.; Ockwig, N. W.; Chae, H. K.; Eddaoudi, M.; Kim, J. *Nature (London, United Kingdom)* **2003**, *423*, 705.

(33) James, S. L. *Chemical Society Reviews* **2003**, *32*, 276.

(34) Kesanli, B.; Lin, W. *Coordination Chemistry Reviews* **2003**, *246*, 305.

(35) Xiao, B.; Yuan, Q. C. *Particuology* **2009**, *7*, 129.

(36) Collins, D. J.; Zhou, H.-C. *J Mater Chem* **2007**, *17*, 3154.

(37) Wood, C. D.; Tan, B.; Trewin, A.; Niu, H.; Bradshaw, D.; Rosseinsky, M. J.; Khimyak, Y. Z.; Campbell, N. L.; Kirk, R.; Stoeckel, E.; Cooper, A. I. *Chemistry of Materials* **2007**, *19*, 2034.

(38) McKeown, N. B.; Budd, P. M.; Book, D. *Macromolecular Rapid Communications* **2007**, *28*, 995.

(39) McKeown, N. B.; Gahnem, B.; Msayib, K. J.; Budd, P. M.; Tattershall, C. E.; Mahmood, K.; Tan, S.; Book, D.; Langmi, H. W.; Walton, A. *Angewandte Chemie, International Edition* **2006**, *45*, 1804.

(40) McKeown, N. B. *Phthalocyanine Materials: Structure, Synthesis and Function*, 1998.

(41) McKeown, N. B. *J Mater Chem* **2000**, *10*, 1979.

(42) Budd, P. M.; Butler, A.; Selbie, J.; Mahmood, K.; McKeown, N. B.; Ghanem, B.; Msayib, K.; Book, D.; Walton, A. *Phys Chem Chem Phys* **2007**, *9*, 1802.

(43) McKeown, N. B.; Budd, P. M. *Macromolecules* **2010**, *43*, 5163.

(44) Davankov, V. A.; Rogozhin, S. V.; Tsyurupa, M. P.; (Institute of Heteroorganic Compounds, Academy of Sciences, U.S.S.R.). Application: DE
DE, 1971, p 15 pp.

(45) Davankov, V. A.; Tsyurupa, M. P. *Reactive Polymers* **1990**, *13*, 27.

(46) Belyakova, L. D.; Kurbanbekov, E.; Larionov, O. G.; Tsyurupa, M. P.; Davankov, V. A. *Russian Chemical Bulletin (Translation of Izvestiya Akademii Nauk, Seriya Khimicheskaya)* **1999**, *48*, 1484.

(47) Tsyurupa, M. P.; Davankov, V. A. *Reactive & Functional Polymers* **2006**, *66*, 768.

(48) Tsyurupa, M. P.; Davankov, V. A. *Reactive & Functional Polymers* **2002**, *53*, 193.

(49) Ahn, J.-H.; Jang, J.-E.; Oh, C.-G.; Ihm, S.-K.; Cortez, J.; Sherrington, D. C. *Macromolecules* **2006**, *39*, 627.

(50) Buda, C.; Dunietz, B. D. *J Phys Chem B* **2006**, *110*, 10479.

(51) Rowsell, J. L. C.; Eckert, J.; Yaghi, O. M. *J Am Chem Soc* **2005**, *127*, 14904.

(52) Lochan, R. C.; Head-Gordon, M. *Phys Chem Chem Phys* **2006**, *8*, 1357.

(53) Turner, S. R.; Anderson, C. C.; Kolterman, K. M. *Journal of Polymer Science, Part C Polymer Letters* **1989**, *27*, 253.

(54) Li, Y.; Turner, S. R. *European Polymer Journal* **2010**, *46*, 821.

(55) Sugihara, T.; Satoh, T.; Miura, M.; Nomura, M. *Angew Chem Int Edit* **2003**, *42*, 4672.

(56) Cava, M. P.; Deana, A. A.; Muth, K.; Mitchell, M. J. *N-Phenylmaleimide*; John Wiley & Sons, Inc., 2008; Vol. 41.

(57) Bicak, N.; Gazi, M.; Karagoz, B. *Designed Monomers and Polymers* **2006**, *9*, 193.

(58) Pyriadi, T. M.; Harwood, H. J. *Polymer Preprints (American Chemical Society, Division of Polymer Chemistry)* **1970**, *11*, 60.

(59) Ventura, B.; Flamigni, L.; Marconi, G.; Lodato, F.; Officer, D. L. *New Journal of Chemistry* **2008**, *32*, 166.

(60) Lijanova, I. V.; Berestneva, T. K.; Garcia, M. M. *Supramolecular Chemistry* **2007**, *19*, 655.

(61) Cavallini, G. M., E.; Nardi, D. *Farmaco, Edizione Scientifica* **1956**, *11*, 378.

(62) Pogorelic, I.; Filipan-Litvic, M.; Merkas, S.; Ljubic, G.; Cepanec, I.; Litvic, M. *Journal of Molecular Catalysis A Chemical* **2007**, *274*, 202.

(63) Mizawa, T.; Takenaka, K.; Shiomi, T. *Journal of Polymer Science, Part A Polymer Chemistry* **2000**, *38*, 237.

(64) Mintz, M. J.; Walling, C. *Org. Synth.* **1969**, *49*.

(65) Odian, G. *Principles of polymerization*, 2004.

(66) Asua, J. M. *Polymer reaction engineering*, 2007.

(67) In http://otech7.tuwien.ac.at/susppoly_sk_e.html.

(68) Mao, M.; Kim, C.; Wi, S.; Turner, S. R. *Macromolecules (Washington, DC, U. S.)* **2008**, *41*, 387.